Anfossi, D. and W. Physick (2004) *Lagrangian Particle Models.* Chapter 11 of *AIR QUALITY MODELING – Theories, Methodologies, Computational Techniques, and Available Databases and Software. Vol. II – Advanced Topics* (P. Zannetti, Editor). Published by The EnviroComp Institute (http://www.envirocomp.org/) and the Air & Waste Management Association (http://www.awma.org/).

Chapter 11

Lagrangian Particle Models

Domenico Anfossi [(1)] and William Physick [(2)]

[(1)] *CNR - Istituto di Scienze dell'Atmosfera e del Clima, Corso Fiume 4, I-10133 Torino (Italy)*
anfossi@isac.cnr.it
[(2)] *CSIRO Atmospheric Research, Private Bag No. 1, Aspendale Vic. 3195 (Australia)*
bill.physick@dar.csiro.au

Contributors:
Gervasio Degrazia [(1)], Enrico Ferrero [(2)(3)], Mark Hibberd [(4)], Peter Hurley [(4)], Ashok Luhar [(4)], Silvia Trini Castelli [(2)(3)], Han Van Dop [(5)]

[(1)] *Universidade Federal de Santa Maria, Departamento de Física, 97105.900 Santa Maria, RS (Brazil)*
[(2)] *Dipartimento di Scienze e Tecnologie Avanzate, Universita' del Piemonte Orientale "A. Avogadro", Corso Borsalino 54, I-15100 Alessandria (Italy)*
[(3)] *ICNR - Istituto di Scienze dell'Atmosfera e del Clima, Corso Fiume 4, I-10133 Torino (Italy)*
[(4)] *CSIRO Atmospheric Research, Private Bag No. 1, Aspendale Vic. 3195 (Australia)*
[(5)] *Institute for Marine and Atmospheric Research, Utrecht P.O. box 80.005 3508 TA Utrecht (The Netherlands)*

Abstract: Lagrangian particle dispersion models are being increasingly used to simulate air pollution dispersion at different spatial and temporal scales and in various stability conditions. In this Chapter, a review of the present state of the art of Lagrangian stochastic models for the description of airborne dispersion in the Planetary Boundary Layer is presented. These models are based on the generalised Langevin equation. Their theoretical basis and relevant implementation aspects are reviewed, and examples of main applications are discussed.

Key Words: Lagrangian air pollution modelling, Langevin equation, stochastic models, mesoscale dispersion, footprint analysis, long-range transport.

1 The Lagrangian Approach (W. Physick, D. Anfossi)

Basically two kinds of models are available to numerically simulate air pollution dispersion: Eulerian models and Lagrangian models. The main difference between the Eulerian and Lagrangian view is that the Eulerian reference system is fixed (with respect to the earth) while the Lagrangian reference system follows the instantaneous fluid velocity.

In a Lagrangian stochastic model (LSM), also called Lagrangian Particle or Random Walk model, the motion of air masses or particles passively following the flow is studied. To simulate the presence of turbulent eddies, particle velocities are subject to a random forcing. Consequently, these models are of stochastic type. The fictitious particles (computer-particles), which represent pollutant gases or aerosols, are considered small enough to follow the motion of smallest eddies and, at the same time, big enough to contain a large number of molecules. Each particle is moved, at each time step, by transport, due to the mean wind, and diffusion, related to the turbulent wind velocity fluctuations.

In the single particle models considered here, the trajectory of each particle represents an individual statistical realisation in a turbulent flow characterised by certain initial conditions and physical constraints. Thus the motion of any particle is independent of the other particles, and consequently the concentration field must be interpreted as an ensemble average. The basic relationship, for an instantaneous source located at x_0 (Csanady, 1973) is:

$$C(x,t) = Q\,P(x,t \mid x_0, t_0) \tag{1}$$

where C is the concentration at time t and location x, Q is the emitted mass at time $t = 0$ and $P(x,t|x_0, t_0)$ is the probability that a particle that was at x_0 at time t_0 arrives at x at time t. To compute $P(x,t|x_0, t_0)$ it is necessary to release a large number of particles, to follow their trajectories and to calculate how many of them arrive in a small volume surrounding x at time t. It is worth noting that particles move in the computational domain without any grid, using as input the values of the first two or three (sometimes four) moments of the probability density distribution (PDF) of wind velocity at the location of the particle. This input information comes either from measurements or from parameterisations

appropriate to the actual stability conditions (unstable, neutral, stable), to the type of site (flat or complex terrain, coast, etc.), and to the time and space scales considered.

This review covers various aspects of LSM derivation and applications. In Section 2 we describe the theoretical basis of LSMs (Langevin equation, Fokker-Plank equation, PDFs, turbulence parameterisation) and present the related technical information (link with meteorological models, boundary conditions, concentration calculation). Particular topics that can be covered within the framework of LSMs (plume rise, reactive chemistry and the prediction of higher order concentration moments) are also included. Section 3 deals with the application of LSMs under various conditions.

2 Lagrangian Stochastic Models (LSM)

2.1 Historical Development (D. Anfossi)

LSMs are mainly based on the generalised Langevin equation for particle velocity. LMS models based on the Langevin equation for particle position also exist, but do not have wide use and we do not discuss them in the present review. Before describing this equation and discussing its details, it may be worthwhile to briefly recall the historical milestones of its derivation (Gardiner, 1990, Rodean, 1996; Anfossi, 2000). The first one was the 1905 Einstein paper on the explanation of Brownian motion. In this paper the concept of stochastic modelling of natural phenomena was introduced for the first time. The main result was that the root-mean-square value of the displacement of the substance particles contained in the flow, under the assumption that successive displacements are independent from the previous ones, is proportional to the square root of the time as diffusion proceeds. Three years later, 1908, Langevin proposed an alternate method to explain the Brownian motion. His method was based on the derivation of an equation, named after him, in which it is assumed that two forces act on each particle: a deterministic one representing the viscous drag and a stochastic one accounting for the random impacts of the other molecules of the liquid. The original Langevin equation reads:

$$\frac{dv}{dt} = -\beta v + \lambda\,\mu(t) \qquad (2)$$

where v is the velocity, t is the time, μ is a random function, and β and λ are two constants. Obviously, in later applications to atmospheric turbulent dispersion, the two terms on the r.h.s. of equation (2) represent the friction force exerted by the flow on the particle (the deterministic term) and the accelerations caused by pressure fluctuations (the stochastic term).

Equation (2) was the first example of a stochastic differential equation. A complete and rigorous treatment of such class of equations was not available until

the nineteen fifties. In particular, when manipulating stochastic equations, it should be noted that $[\mu(t)]^2$ is of the order dt and so cannot be neglected in comparison with dt. Consequently, the usual "function of a function" derivation rule must be substituted by Ito's formula that prescribes that the derivative of a stochastic function of velocity and position $f(x,u)$ is:

$$d[f(x,u)] = \left(u\frac{\partial f}{\partial x} + a\frac{\partial f}{\partial u} + b\frac{\partial^2 f}{\partial u^2} \right) dt + b\frac{\partial f}{\partial u} d\mu \tag{3}$$

where *a* and *b* are functions of *x* and *u*.

The Langevin equation is a Lagrangian equation. Its corresponding Eulerian equation is the Fokker-Planck equation derived in the years 1915-1917. The diffusion equation written by Einstein in his 1905 derivation is a special case of the Fokker-Planck equation. Taylor (1921) considered correlated particle displacements and obtained the fundamental results that the mean-square value of the displacement is proportional to the time elapsed from the emission in the first phase of the diffusion process and is proportional to the square root of time for longer times, thus recovering, in this second limit, the Einstein result. Obukhov (1959) first proposed that the evolution of the motion of an air particle in the atmosphere be described as a Markov process. Smith (1968) assumed that the Lagrangian turbulent fluctuation of a given parcel velocity at time $t+\tau$, $v'(t+\tau)$, is related to the same quantity at time t, $v'(t)$, according to the following relationship:

$$v'(t+\tau) = v'(t)R(\tau) + v''(t) \tag{4}$$

in which $R(\tau)$ is the autocorrelation coefficient at time lag τ and $v''(t)$ is a random velocity fluctuation, assumed independent of $v'(t)$. Both equations (2) and (4) assume stationary and homogeneous turbulence. It is interesting to point out the relation between these two equations. The second one can be considered either the finite difference form of the first one (Sawford, 1985; Gifford, 1982), or it can be obtained by integrating the first one with respect to time (Legg and Raupach, 1982). On the other hand, equation (2) can be derived from equation (4) by combining the latter with its Taylor series expansion and dropping higher order terms (Gaffen et al., 1987; Durbin and Petterson Reif, 2001).

Hanna (1979) showed, by direct comparison with atmospheric Eulerian and Lagrangian turbulence data, that equation (4) is approximately valid, and therefore applicable, in the PBL.

Since the nineteen seventies, many pioneering papers (see, for instance: Reid, 1979; Zannetti, 1981, 1984; Ley, 1982; Davis, 1983) have appeared in the

literature aimed at simulating atmospheric turbulent dispersion by means of the Langevin equation, written as follows:

$$dv' = -\frac{v'}{T_L}dt + \sigma_v\left(\frac{2}{T_L}\right)^{\frac{1}{2}}d\mu \tag{5}$$

or in its finite difference form (equation 4), where T_L is the Lagrangian time scale and σ_v is the velocity standard deviation. Zannetti (1981, 1984), in particular, proposed the first model that considered all the correlations among the three wind components.

However, it became immediately clear that equation (5) could not be applied in non-homogeneous turbulence, because it leads to accumulation of particles in the regions where σ_v is small. This is an important point, since vertical turbulence conditions in the PBL are never homogeneous. In neutral stability, turbulence is non-homogeneous but, generally, Gaussian. In convective conditions turbulence is neither homogeneous nor Gaussian. This problem was examined by, among others, Wilson et al. (1981), Legg and Raupach (1982) and Sawford (1985) who attributed the accumulation to a mean drift velocity induced by the gradient in vertical velocity variance. A proposed drift term correction to the r.h.s. of equation (5), for the vertical component, generally had the following expression: $1/2\left(1+w'^2/\sigma_w^2\right)\partial\sigma_w^2/\partial z\,dt$ This was used with success, for instance, by Brusasca et al. (1989). Since then, in the literature, particular attention has been paid to dispersion in convective conditions. In these conditions, the vertical velocity PDF is not Gaussian, due to the presence of updrafts and downdrafts, and, as a consequence, it is necessary to take into account at least the third order moment of the vertical velocity fluctuations. With relation to this problem, important contributions were given by the basic papers due to Baerentsen and Berkowicz (1984), Thomson (1984), Van Dop et al., 1985 and De Baas et al. (1986) which introduced the treatment of updrafts and downdrafts and, therefore, of skewed PDFs, into the Langevin equation, obtaining realistic and physically correct simulations of dispersion in convective conditions (see section 3). The test database, widely used by the international community, was due to Willis and Deardorff (1976, 1978 and 1981) who performed very skilful and comprehensive water tank tracer dispersion experiments.

The conclusive paper, at least for the moment, defined by Rodean (1996) as a "classical landmark paper", was due to Thomson (1987). He demonstrated that by using the “well-mixed condition” (particles that are initially uniformly distributed in space, must remain so and they have the same velocity distribution as the fluid) as the criterion for selecting the correct model for the diffusion of scalars in a turbulent flow, the atmospheric dispersion of pollutants can be successfully simulated with LSMs based on a generalised form of the Langevin equation. This form is capable of representing skewed inhomogeneous non-stationary conditions, without adding any "ad hoc" drift correction term, and incorporates an exact

formulation of non-Gaussian turbulence. Also, unlike in previous versions of the Langevin equation, it is not necessary to incorporate the skewness of the CBL in the random term, which remains Gaussian.

2.2 Theory (E. Ferrero)

LSMs are based on the Langevin equation that describes the temporal evolution of the velocity of pollutant particles in a turbulent field. The solution of the Langevin equation is a continuous stochastic Markov process. In fact, particle position and velocity, in a turbulent flow, can be considered a bivariate Markov process in the range of the turbulent energy spectrum between the Kolmogorov time scale τ_n (approximately equal to the correlation time of the accelerations) and the velocity correlation Lagrangian time scale T_L.

The Langevin equation for the turbulent velocity can be written as follows:

$$du_i(t) = a_i(\vec{x},\vec{u},t)\cdot dt + b_{i,j}(\vec{x},\vec{u},t)\cdot dW_j \tag{6}$$

and is coupled to the equation for the position x(t):

$$dx_i(t) = u_i(t)\cdot dt \tag{7}$$

where $d\vec{W}$ is an incremental Wiener process that is Gaussian with zero mean and a variance of:

$$\left\langle dW_i(t)\cdot dW_j(t')\right\rangle = \delta_{ij}\delta(t-t')\cdot dt\cdot dt'$$

where the notation < > represents an ensemble average.

The term $b_{i,j}(\vec{x},\vec{u},t)\cdot$ can be derived from the Kolmogorov theory of local isotropy in the inertial sub-range (Monin and Yaglom, 1975). This theory is based on similarity relations valid in a particular interval of the turbulence spectrum. The energy is transferred from the larger vortices to the smaller ones, until to the smallest scales of the atmospheric turbulence, where it is dissipated by the viscosity. Inside this energetic cascade there is a part of the spectrum where the vortices are sufficiently small so that they are not affected by the anisotropy induced from the larger vortices and are not dissipated as heat. This part of the turbulent spectrum is called the inertial sub-range. This interval coincides with the interval of temporal scales in which the turbulent velocities can be considered a Markov process.

Defining the structure function of the Lagrangian velocities, in one dimension, as:

$$D = \left\langle \left(u_i(t) - u_i(t+dt)\right)^2 \right\rangle = \left\langle du_i(t)^2 \right\rangle \tag{8}$$

then, if $\tau_n \leq dt \leq T_L$, the following relationship can be considered:

$$D = C_0 \cdot \varepsilon \cdot dt$$

where ε is the dissipation rate of turbulent kinetic energy and C_0 is a universal constant.

Substituting $du_i(t)$, as given by the Langevin equation, in (8), averaging and considering only the terms of the order of dt, leads to:

$$D = \left\langle du_i{}^2 \right\rangle = b_{ij}{}^2 \cdot \left\langle dW_i{}^2 \right\rangle = b_{ij}{}^2 dt = \delta_{ij} C_0 \cdot \varepsilon \cdot dt$$

and

$$b_{ij} = \delta_{ij} \sqrt{C_0 \cdot \varepsilon} \tag{9}$$

An Eulerian description of a continuous Markov process is available through the Fokker-Planck equation. If the position and turbulent velocity can be considered a continuous stochastic Markov process, the Fokker-Planck equation can be used to calculate the coefficient $\vec{a}$ of the Langevin equation for any given probability density function (PDF) (Gardiner, 1990).

$$\frac{\partial P\left(\vec{x},\vec{u},t\right)}{\partial t} + \frac{\partial}{\partial x_i}\left(u_i\left(\vec{x},t\right)\cdot P\left(\vec{x},\vec{u},t\right)\right) = -\frac{\partial}{\partial u_i}\left(a_i\left(\vec{x},\vec{u}\right)\cdot P\left(\vec{x},\vec{u},t\right)\right) + \frac{1}{2}\cdot\frac{\partial^2}{\partial u_i u_j}\left(b_{ij}{}^2\left(\vec{x}\right)\cdot P\left(\vec{x},\vec{u},t\right)\right)$$

where $P\left(\vec{x},\vec{u},t\right)$ is the Eulerian PDF of the particles.

In the stationary case, $P\left(\vec{x},\vec{u},t\right)$ does not depend on time and the Fokker-Planck equation reduces to:

$$\frac{\partial}{\partial x_i}\left(u_i\left(\vec{x}\right)\cdot P\left(\vec{x},\vec{u}\right)\right)= -\frac{\partial}{\partial u_i}\left(a_i\left(\vec{x},\vec{u}\right)\cdot P\left(\vec{x},\vec{u}\right)\right)+\frac{1}{2}\cdot\frac{\partial^2}{\partial u_i u_j}\left(b_{ij}{}^2\left(\vec{x}\right)\cdot P\left(\vec{x},\vec{u}\right)\right) \tag{10}$$

where b_{ij} is given by (9).

Following Thomson (1987), it can be stated that an LSM satisfies the well-mixed condition (if the particles are initially well-mixed in the fluid, they will remain so), if $P\left(\vec{x},\vec{u}\right)$ is equal to the Eulerian *atmospheric* PDF. This is a necessary and sufficient condition. In other words all moments of $P\left(\vec{x},\vec{u}\right)$ must equal the measured or parameterised moments.

In one dimension, the Fokker-Planck equation can be solved and the term *a(x,u)* calculated, for a given PDF, as follows (Thomson, 1987):

$$a(x,u)=\frac{1}{P(x,u)}\cdot\left(\frac{C_0\varepsilon}{2}\cdot\frac{\partial P(x,u)}{\partial u}+\phi(x,u)\right) \tag{11}$$

where

$$\phi(x,u)=-\frac{\partial}{\partial x}\cdot\int_{-\infty}^{u}u\cdot P(x,u)\cdot du \tag{12}$$

and

$$\phi\to 0 \quad per \quad |u|\to\infty$$

In addition (Hinze, 1975; Tennekes, 1982; Rodean, 1994; Luhar and Britter, 1989; Weil, 1990; Reynolds 1998),

$$\frac{C_0\varepsilon}{2}=\frac{\sigma^2}{T_L} \tag{13}$$

LSMs usually are one-dimensional models solving one or two and, in some cases, three Langevin equations, one for each Cartesian direction. The extension to a fully three dimensional model was dealt with by Sawford and Guest (1988), Sawford (1993) and Borgas and Sawford (1994). It can be demonstrated that a unique solution for the Fokker-Planck equation, in the three-dimensional case, exists only for homogeneous, isotropic turbulence (Borgas and Sawford, 1994).

The non-uniqueness of the 2D and 3D solution is related to the first term on the right side of (10), as this equation can be satisfied by any vector obtained through adding a rotational vector, in $\vec{u}$ space, to $\vec{a}$ P (Sawford, 1993; Rotach et al., 1996).

Concerning the value of the basic constant C_0, different values can be found in literature, mainly ranging from about 2 to 4 (Luhar and Britter, 1989; Hurley and Physick, 1991 and 1993; Physick et al., 1994; Tassone et al., 1994; Rotach et al., 1996; Degrazia and Anfossi 1998). Sawford (1991) showed that C_0 is a function of the Reynolds number based on the Eulerian Taylor microscale, Re_λ. C_0 reaches an asymptotic value, C_0 =7, for growing Re_λ. The variability in the value of this constant was discussed by Du (1997), who suggested that it can be related to the method used for estimating C_0 and proposed the value 3.0 ± 0.5 for using in Lagrangian Stochastic models, in neutral conditions. Reynolds (1998) demonstrated that the value 5.0 ± 0.5 gives satisfactory results in simulating a wind tunnel boundary layer and suggested that one-dimensional Lagrangian stochastic models are inconsistent with the supposed universality of C_0. Anfossi et al. (2000), by analysing turbulence observations, made in the surface layer, under unstable conditions by a sonic anemometer, found C_0 = 4.3 for the crosswind and vertical turbulent velocity components and C_0 = 3.2 for the longitudinal one. According to these authors, the partitioning of C_0 in different spatial components is a consequence of the directional dependence of the Eulerian correlation functions due to the local isotropy in the inertial sub-range.

Stohl and Thomson (1999) stressed the effects of the density variation in the boundary layer and proposed a density correction term. They also demonstrated that this term influences the surface concentration.

The theory of this section is applicable to one-particle models, and these have been widely tested and applied to many different situations characterised by non-homogeneous turbulence and different stability conditions (see section 3). However, it should be stressed that a one-particle model is only able to describe the absolute dispersion and to predict the mean concentration fields. When one is interested in the relative dispersion and mean-square concentration field, a two-particle model should be developed and applied (Durbin, 1980), although recently one-particle Lagrangian models have been used in conjunction with the meandering plume approach of Gifford (1959) to determine higher order concentration fluctuation statistics for practical applications (Section 20). In the two-particle case the assumption of Markovian and continuous process should be made jointly for the positions and velocities of the particles pair (Thomson, 1990; Sawford, 1993; Borgas and Sawford, 1994). An important advantage of the two-particle model is the ability to include second order chemical reaction (Crone et al. 1999). Unfortunately, in the case of the two-particle model, a unique solution of the Fokker-Planck equation does not exist even in isotropic turbulence, in the fully three-dimensional case (Sawford, 1993).

A hybrid LSM, referred to as the PARTPUFF (Hurley, 1994), was designed to save computer time for high horizontal-resolution simulations. This model employs the LSM approach in the vertical direction, and a Gaussian puff approach in the horizontal directions. This method allows a particle/puff to influence more than one horizontal grid-point, enabling a reduction in the number of particles needed in a simulation. A related approach in which puffs and particles are combined is described by De Haan and Rotach (1998).

2.3 Choice of Eulerian PDF (E. Ferrero, D. Anfossi, M. Hibberd)

The main input of physical data to LSMs is through the PDF of Eulerian turbulent velocities (see 10), the form of which depends on the prevailing turbulence characteristics. If this PDF is Gaussian, it can be fully described by the mean and standard deviation, otherwise higher order moments are also needed. For actual atmospheric PDFs, their non-Gaussian form can usually be described sufficiently accurately by adding moments up to third or fourth order.

Since most LSM applications concern vertical dispersion in the convective boundary layer (CBL), we will mainly focus on this kind of dispersion. In convective conditions the vertical velocity PDF is asymmetric and, as a consequence, to correctly describe dispersion, it is necessary to prescribe an analytical expression for the PDF based on the measured higher order moments of Eulerian vertical velocity fluctuations.

In this section we present PDFs that are most commonly used in LSMs: Gaussian, bi-Gaussian and Gram-Charlier. The various closure schemes used with the bi-Gaussian PDF form are described. Advantages of analytical solutions and approaches other than closure (such as using a quadratic form for the acceleration term in the stochastic equation) are discussed.

2.3.1 Gaussian PDF

In homogeneous turbulence the PDF of velocity fluctuations is assumed to be Gaussian. This assumption may also be made for inhomogeneous Gaussian turbulence, which, for example, is a good first approximation for the neutral PBL. This choice implies that the generalised Langevin equation (see equation 6) in inhomogeneous conditions, without the Reynolds stress terms, reduces to the following form for each component (Rodean, 1996):

$$du_i = -\frac{u_i}{T_{Li}}dt + \frac{1}{2}\left[1+\left(\frac{u_i}{\sigma_{ui}}\right)^2\right]\frac{\partial\sigma_{ui}^2}{\partial x_i}dt + \sigma_{ui}\left(\frac{2}{T_{Li}}\right)^{\frac{1}{2}}d\mu \qquad (14)$$

This equation was first proposed by Wilson et al. (1983) and rigorously derived by Thomson (1987). In homogeneous turbulence equation (14) further reduces to:

$$du_i = -\frac{u_i}{T_{Li}}dt + \sigma_{ui}\left(\frac{2}{T_{Li}}\right)^{\frac{1}{2}} d\mu \tag{15}$$

This equation is identical to equation (5).

2.3.2 Bi-Gaussian PDF

Pearson (1894) was the first to suggest the use of linear combinations of normal distributions for fitting observed frequency distributions having a non-Gaussian shape, for example

$$P(w,z) = A \cdot P_A(w_a, \sigma_A) + B \cdot P_B(w_B, \sigma_B) \tag{16}$$

where A+B=1, $A > 0$, $B > 0$ and P_A and P_B are Gaussian PDFs with means w_A, w_B, and standard deviations σ_A, σ_B.

Baerentsen and Berkowicz (1984) first introduced this PDF into LSMs, where the Gaussian PDFs have the form

$$P_A = \left[(2\pi)^{1/2}\sigma_A\right]^{-1} \exp\left[-(w - w_A)^2 / (2\sigma_A^2)\right] \tag{17}$$

and similarly for P_B. (Note that there is a potential for confusion when using equations given in the literature because some authors use absolute values of the means in the PDF expressions rather than their signed values.) The values of the parameters (A, B, w_A, w_B, σ_A, σ_B) are obtained from the definition of the moments of the distribution:

$$\overline{w^n} = A \cdot \int_{-\infty}^{+\infty} w^n \cdot P_A(w,z) \cdot dw + B \cdot \int_{-\infty}^{+\infty} w^n \cdot P_B(w,z) \cdot dw \tag{18}$$

where $\overline{w^n}$ are the measured or parameterised moments of the atmospheric PDF. In principle, the six unknowns can be determined by solving the zeroth to fifth order moment equations. However, the absence of data for the highest moments makes it more practical to use just the first few moments and to make some closure assumption. Writing out Equation (18) for the first four moments leads to the following system of equations:

$$\begin{aligned} A + B &= 1 \\ Aw_A + Bw_B &= \overline{w} = 0 \\ A\left(w_A{}^2 + \sigma_A{}^2\right) + B\left(w_B{}^2 + \sigma_B{}^2\right) &= \overline{w^2} \\ A\left(w_A{}^3 + 3w_A\sigma_A{}^2\right) + B\left(w_B{}^3 + 3w_B\sigma_B{}^2\right) &= \overline{w^3} \\ A\left(w_A{}^4 + 6w_A{}^2\sigma_A{}^2 + 3\sigma_A{}^4\right) + B\left(w_B{}^4 + 6w_B{}^2\sigma_B{}^2 + 3\sigma_B{}^4\right) &= \overline{w^4} \end{aligned} \tag{19}$$

Baerentsen and Berkowicz (1984) considered the first three moments and used the closure assumption

$$\sigma_A = |w_A| \quad \sigma_B = |w_B| \tag{20}$$

to solve for the parameters:

$$\begin{aligned} w_B &= \frac{\overline{w^3} - \sqrt{\left(\overline{w^3}\right)^2 + 8 \cdot \left(\overline{w^2}\right)^3}}{4 \cdot \overline{w^2}}, \quad w_A = -\overline{w^2} / 2\overline{w_B}\ , \\ A &= \frac{w_B}{w_B - w_A}, \quad B = 1 - A \end{aligned} \tag{21}$$

This system of equations has probably been the most widely employed of the closures described here, although some of the other closures give better results. Using this closure (20) with equation (16) for the PDF in the Fokker-Planck equation (equations 10 and 12), Luhar and Britter (1989) obtained an explicit expression for Φ. The general expression for Φ in their model is:

$$\begin{aligned} \phi \ = AP_A & \left[\frac{\sigma_A^2}{A}\frac{\partial A}{\partial z} + \frac{\partial \sigma_A}{\partial z}\left(\sigma_A + \frac{w\left(w - w_A\right)}{\sigma_A}\right) + w\frac{\partial w_A}{\partial z} \right] + \\ & \frac{1}{2}\frac{\partial\left(Aw_A\right)}{\partial z}\left[1 - erf\left(\frac{w - w_A}{\sqrt{2}\sigma_A}\right)\right] + \\ & BP_B\left[\frac{\sigma_B^2}{B}\frac{\partial B}{\partial z} + \frac{\partial \sigma_B}{\partial z}\left(\sigma_B + \frac{w\left(w - w_B\right)}{\sigma_B}\right) + w\frac{\partial w_B}{\partial z} \right] + \\ & \frac{1}{2}\frac{\partial\left(Bw_B\right)}{\partial z}\left[1 - erf\left(\frac{w - w_B}{\sqrt{2}\sigma_B}\right)\right] \end{aligned} \tag{22}$$

,

where erf(z), the error function, is defined as:

$$erf\left(z\right) = \frac{2}{\sqrt{\pi}} \cdot \int_0^z \exp\left(-s\right) \cdot ds$$

and any closure assumption can be substituted in Equation (22).

Weil (1990) generalised the Baerentsen and Berkowicz (1984) closure assumption to:

$$\sigma_A = R\left|w_A\right| \quad \text{and} \quad \sigma_B = R\left|w_B\right|, \tag{23}$$

and obtained solutions:

$$w_A = \frac{1}{2}\sqrt{\overline{w^2}}\left[\alpha S + \left(\alpha^2 S^2 + \frac{4}{\beta}\right)^{\frac{1}{2}}\right], \quad w_B = \frac{1}{2}\sqrt{\overline{w^2}}\left[\alpha S - \left(\alpha^2 S^2 + \frac{4}{\beta}\right)^{\frac{1}{2}}\right] \tag{24}$$

where:

$$S = \frac{\overline{w^3}}{\left(\overline{w^2}\right)^{\frac{3}{2}}}, \quad \alpha = \frac{1+R^2}{1+3R^2} \quad \text{and} \quad \beta = 1+R^2$$

S is the skewness. Weil used a value of R =3/2. The Eulerian PDF generated using this closure assumption has been found to lead to good agreement with point source dispersion results in the CBL and is recommended over the Baerentsen and Berkowicz (1984) form (Luhar at al, 1996).

Du et al. (1994) considered all four moments listed in equations (19) with A=0.4 and the Gaussian value of 3 assumed for the kurtosis $K\left(=\overline{w^4}\Big/\overline{w^2}^2\right)$:

$$\overline{w^4} = 3\left(\overline{w^2}\right) \tag{25}$$

They obtained

$$w_A = \left(\overline{w^3}\right)^{1/3}, \; w_B = -\frac{2}{3}\left(\overline{w^3}\right)^{1/3}$$

$$\sigma_A = \left[\overline{w^2} - 0.280\left(\overline{w^3}\right)^{2/3}\right]^{1/2}, \quad \sigma_B = \left[\overline{w^2} - 0.927\left(\overline{w^3}\right)^{2/3}\right]^{1/2} \tag{26}$$

Equations (26) yield real solutions for $S \le 1.12$.

Another closure for the bi-Gaussian PDF that includes up to the fourth moment was proposed by Anfossi et al. (1996). They suggested two different closures without assuming any a priori value for $\overline{w^4}$. The first closure assumed $\sigma_A = \sigma_B = \sigma$ and the second closure set A = B = ½. Both PDFs had restrictions on the range of skewness S and kurtosis K to ensure real solutions were obtained.

A comparison among different closures performed by Ferrero et al. (1998b) in CBL dispersion showed that these closures perform as well as the one by Du et al. (1994) but generally less well than the one by Baerentsen and Berkowicz (1984) and the Gram Charlier method (described below).

The closure assumptions considered so far are not well behaved as the skewness approaches zero, i.e. they do not collapse to a simple Gaussian PDF. In order to overcome this problem, Luhar et al. (1996) proposed a more generalised form of Weil's (1990) closure, based on the skewness value *S*:

$$w_A = m\,\sigma_A, \qquad w_B = -\,m\,\sigma_B, \quad m = (2/3)\,S^{1/3} \tag{27}$$

This has the correct property that the bi-Gaussian PDF collapses to a Gaussian PDF in the zero skewness limit and so can be used to investigate the influence of skewness on dispersion in the CBL. It gives the following values for the parameters

$$\sigma_A = \sqrt{\overline{w^2}}\left[\frac{B}{A\left(1+m^2\right)}\right]^{1/2}, \quad \sigma_B = \sqrt{\overline{w^2}}\left[\frac{B}{B\left(1+m^2\right)}\right]^{1/2}$$

$$A = \frac{1}{2}\left[1-\left(\frac{r}{4+r}\right)^{1/2}\right], \quad B = 1-A, \tag{28}$$

where

$$r = \left[\left(1+m^2\right)^3 S^2\right] \Big/ \left[\left(3+m^2\right)^2 m^2\right]$$

and the kurtosis is given by

$$K = (1+r)\left(3+6m^2+m^4\right) \Big/ \left(1+m^2\right)^2$$

Luhar et al. (1996) reported that the 2/3 constant in equation (27) was chosen to best match the observed values for the higher moments of $S = 0.8$ and $K = 3.9$ in most of the CBL. Comparison with laboratory experiments of Hibberd and Sawford (1994) showed that this closure produced similar CBL dispersion results to those obtained with the Weil (1990) closure, and better than those of Baerentsen and Berkowicz (1984) and Du et al. (1994).

The model of Rotach et al. (1996) has also the property that it has a skewed PDF for convective conditions and is 'well behaved' in the Gaussian limit. As an additional advantage it is more than one-dimensional, i.e. it includes the effect of velocity covariances

Wilson and Flesch (1993) warn of the risk of numerical underflows/overflows with all these models when evaluating the tails of the exponential distributions; use of double precision and sufficiently small timesteps is recommended.

2.3.3 Gram-Charlier PDF

Most of the closures described so far are based on the idea that A and B in equation (14) may be associated with the fractions of the area occupied by updrafts and downdrafts, w_A and w_B with the mean updraft and downdraft velocities, and σ_A and σ_B with the corresponding variances of the vertical velocity fluctuations. However, De Baas et al. (1986) and Anfossi et al. (1996) note that all these PDFs are just mathematical approximations. It is not necessary that the parameters in the model be directly related to physical quantities. In all cases, it is just the moments of the PDFs that are derived from experimental data.

An alternative form for the PDF proposed by Anfossi et al. (1996) and Ferrero and Anfossi (1998a, b) on the basis of these considerations is the Gram-Charlier PDF. This PDF, truncated to fourth order (GC4), has the following form (Kendall and Stuart, 1977):

$$P(x,z)=\frac{e^{-x^2/2}}{\sqrt{2\pi}}\left(1+C_3H_3+C_4H_4\right) \tag{29}$$

where H_3 and H_4 are Hermite polynomials and C_3 and C_4 their coefficients, whose expressions are:

$$\begin{aligned} H_3 &= x^3-3x & H_4 &= x^4-6x^2+3 \\ C_3 &= \overline{\mu^3}/6 & C_4 &= \left(\overline{\mu^4}-3\right)/24 \end{aligned} \tag{30}$$

and $\overline{\mu^3}$, $\overline{\mu^4}$ are the standardised moments of w and $x = w/\sigma_w$. Solving equation (12) in which P is given by (29), the following expressions are found:

$$\Phi=\frac{1}{2}\frac{\partial\sigma_w^2}{\partial z}\frac{e^{-\frac{x^2}{2}}}{\sqrt{2\pi}}\left[1-C_4+x^2\left(1+C_4\right)-2C_3x^3-5C_4x^4+C_3x^5+C_4x^6\right] \tag{31}$$

and

$$a=\sigma_w\frac{\frac{1}{T_{Lw}}\left(T_1\right)+\frac{\partial\sigma_w}{\partial z}\left(T_2\right)}{T_3} \tag{32}$$

where

$$
\begin{aligned}
T_1 &= -3C_3 - x(15C_4 + 1) + 6C_3x^2 + 10C_4x^3 - C_3x^4 - C_4x^5 \\
T_2 &= 1 - C_4 + x^2(1 + C_4) - 2C_3x^3 - 5C_4x^4 + C_3x^5 + C_4x^6 \\
T_3 &= 1 + 3C_4 - 3C_3x - 6C_4x^2 + C_3x^3 + C_4x^4
\end{aligned}
\tag{33}
$$

We note that a Gram-Charlier distribution truncated to third order (GC3) can be derived from equations (33) simply by setting $C_4 = 0$. If C_3 is also set to zero, equation (29) reduces to the Gaussian PDF. Thus, this PDF also has the correct property of collapsing to a Gaussian PDF when the skewness is equal to zero.

Gram-Charlier series expansions, though showing good correspondence to experiments (see, for instance: Frenkiel and Klebanoff, 1967; Antonia and Atkinson, 1973; Durst et al., 1992; Anfossi et al., 1996) can exhibit small negative probabilities in the tails of the distribution (Frenkiel and Klebanoff,1967; Flesch and Wilson, 1992; Du et al., 1994; Anfossi et al., 1996). Numerical experiments (Ferrero and Anfossi, 1998b) showed that discarding these non-physical probabilities is inconsequential in practical applications because these unrealistic velocities occur so rarely

Advantages of the Gram-Charlier PDFs are their computational efficiency and the ability to include information on the Eulerian moments directly. The GC form also provides greater flexibility in choosing the shape of the PDF to match observations. It has been shown to give good results both in the atmospheric surface layer (Anfossi et al., 1996) and for all stabilities in PBL dispersion (Ferrero and Anfossi, 1998b; Tinarelli et al., 2000).

An alternative way of using the GC PDF was proposed by Tassone et al. (1994). They assumed that the variance of the Gaussian distribution included in the GC PDF (see equation 29) is proportional to, rather than equal to, the second moment of vertical velocity distribution (included in the Hermite polynomials): $\sigma_w^2 = f(z)\overline{w^2}$, where the value of f is determined empirically. By comparing this closure to the Willis and Deardorff (1981) water tank experiments, Vinter Falk (1998) found that the position and size of the ground level concentration peak were well predicted but the right side (positive velocities) of the PDF could present a pronounced non-physical dive in the plume centreline.

2.3.4 Quadratic Form for the Acceleration Term

Franzese et al. (1999) adopted a different approach and assumed that the deterministic acceleration term in the stochastic differential equation can be parameterised as a quadratic function of velocity:

$$a(w,z) = \alpha(z)w^2 + \beta(z)w + \gamma(z) \tag{34}$$

The coefficients are assumed to be height dependent. Their values are determined from the first four moments of the Eulerian velocities with integration of the Fokker-Planck equation.

The main advantage of this approach is its computational efficiency. Test showed that model run times were reduced to a quarter of those for the Luhar and Britter (1989) model. A further advantage is that moments up to fourth order can be used without any predefined form for the PDF. However, the skewness cannot exceed a value of about 0.6, otherwise the model does not produce a vertically well-mixed concentration distribution at large times. This is probably due to the inadequacy of the first few moments for fully describing the physical PDF (Borgas, pers. comm.). In fact, all the methods discussed in this section are approximations to physical PDFs and may fail to properly describe dispersion in particular circumstances.

2.4 Turbulence Parameterisation (G. Degrazia)

A turbulence parameterisation is an approximation to nature in the sense that we are putting in physical models an approximated relation that in principle can be used as a surrogate for the natural true unknown term. The reliability of each model strongly depends on the way turbulent parameters are calculated and related to the current understanding of the PBL. Most of the turbulence parameterisations used in advanced dispersion models are based on PBL similarity theories (Hanna, 1982; Stull, 1988; Holtslag and Moeng, 1991; Kaimal and Finnigan, 1994; Sun, 1993; Rodean, 1994).

Through classical statistical diffusion theory (Batchelor, 1949), it is possible to relate turbulent parameters (wind velocity standard deviations σ_i $(i = u, v, w)$ and Lagrangian decorrelation time scales T_{Li}) to spectral distribution of turbulent kinetic energy (TKE). Following this approach, Hanna (1982) and Degrazia et al. (2000) developed expressions for the Lagrangian decorrelation time scales based on the peak wavelength of the turbulent velocity spectra. These two parameterisations that can be used in Lagrangian stochastic dispersion models are here presented. Parameterisations for the third order moments for the vertical velocity ($\overline{w^3}$) and the dissipation rate (ε) are also presented.

2.4.1 Hanna's Parameterisation

Based on analyses of field experiments (Hanna, 1968; Kaimal et al., 1976,1982; Caughey, 1979; Hanna,1981), theoretical considerations (Panofsky et al.,1977; Irwin, 1979a) and second-order closure model (Wyngaard et al., 1974), Hanna (1982) proposed the following parameterisations:
in the unstable case:

for $\frac{z}{z_i}$<0.03,

$$\sigma_u = \sigma_v = (u_*)_o \left[12 + \frac{1}{2} \frac{z_i}{|L|} \right]^{1/3} \tag{35}$$

$$\sigma_w = 0.96\, w_* \left(3\frac{z}{z_i} - \frac{L}{z_i} \right)^{1/3} \tag{36}$$

for $0.03 < \frac{z}{z_i} < 0.4$

$$\sigma_w = w_* \min\left\{ 0.96\left(3\frac{z}{z_i} - \frac{L}{z_i} \right)^{1/3}, 0.763\left(\frac{z}{z_i} \right)^{0.175} \right\} \tag{37}$$

for $0.4 < \frac{z}{z_i} < 0.96$

$$\sigma_w = 0.722 w_* \left(1 - \frac{z}{z_i} \right)^{0.207} \tag{38}$$

for $0.96 < \frac{z}{z_i} < 1$

$$\sigma_w = 0.37 w_* \tag{39}$$

$$T_{Lu} = T_{Lv} = 0.15 \frac{z_i}{\sigma_u} \tag{40}$$

$$T_{Lw} = 0.1 \frac{z}{\sigma_w} \frac{1}{0.55 + 0.38\left[\frac{(z - z_0)}{L} \right]} \qquad \frac{z}{z_i} < 0.1 \quad \text{and} \quad -\frac{(z - z_0)}{L} < 1 \tag{41}$$

$$T_{Lw} = 0.59\frac{z}{\sigma_w} \qquad \frac{z}{z_i} < 0.1 \quad \text{and} \quad -\frac{(z - z_0)}{L} > 1 \tag{42}$$

$$T_{Lw} = 0.15\frac{z_i}{\sigma_w}\left[1 - \exp\left(-\frac{5z}{z_i}\right)\right] \qquad \frac{z}{z_i} > 0.1 \tag{43}$$

in the stable case:

$$\sigma_u = 2(u_*)_0\left(1 - \frac{z}{h}\right) \quad \text{and} \quad \sigma_w = \sigma_v = 1.3(u_*)_0\left(1 - \frac{z}{h}\right) \tag{44}$$

$$T_{Lu} = 0.15\frac{h}{\sigma_u}\left(\frac{z}{h}\right)^{0.5} ; T_{Lv} = 0.07\frac{h}{\sigma_v}\left(\frac{z}{h}\right)^{0.5} \quad \text{and} \quad T_{Lw} = 0.10\frac{h}{\sigma_w}\left(\frac{z}{h}\right)^{0.8} \tag{45}$$

and in the neutral case:

$$\sigma_u = 2(u_*)_0 \exp\left(-\frac{3f_c z}{(u_*)_0}\right) \quad \text{and} \quad \sigma_w = \sigma_v = 1.3(u_*)_0 \exp\left(-\frac{2f_c z}{(u_*)_0}\right) \tag{46}$$

$$T_{Lu} = T_{Lv} = T_{Lw} = \frac{0.5\dfrac{z}{\sigma_w}}{1 + 15\dfrac{f_c z}{(u_*)_0}} \tag{47}$$

where $(u_*)_0$ is the surface friction velocity; z_i is the Convective Boundary Layer (CBL) height; z is the height above the surface; L is the Monin-Obukhov length; w_* is the convective velocity scale; z_o is the aerodynamic roughness; h is the height of the turbulent stable boundary layer and f_c is the Coriolis parameter ($f_c = 10^{-4} s^{-1}$ in mid-latitudes).

2.4.2 Degrazia et al. Parameterisation

Degrazia et al. (2000) parameterisation is based on Taylor's statistical diffusion theory, in which the shear buoyancy PBL spectra are modelled by means of a linear combination of the convective and mechanical turbulent energy. In this parameterisation the buoyant and mechanical wind turbulent velocity variances $\left(\sigma_{ib}^2, \sigma_{is}^2\right)$ are given by the following expressions:

$$\sigma_{ib}^2 = \int_0^\infty S_{ib}^E(n)dn = \frac{1.06 c_i \psi_\varepsilon^{2/3} w_*^2 \left(\frac{z}{z_i}\right)^{2/3}}{\left[(f_m^*)_i^c\right]^{2/3}} \tag{48}$$

and

$$\sigma_{is}^2 = \int_0^\infty S_{is}^E(n)dn = \frac{2.32 c_i \phi_\varepsilon^{2/3} u_*^2}{\left[(f_m^*)_i^{n+s}\right]^{2/3}} \tag{49}$$

On the other hand, the Lagrangian decorrelation time scale assumes the following expression:

$$T_{Li} = \frac{l_i}{\sigma_i} = \frac{z}{\sqrt{c_i}} \left\{ \frac{0.14 \left(\frac{-\overline{L}}{z_i} \frac{z_i}{-L}\right)^{1/2}}{[(f_m^*)_i^c]^{2/3} \; w_* \left(\psi_\varepsilon \frac{z}{z_i}\right)^{1/3}} + \frac{0.059}{[(f_m^*)_i^{n+s}]^{2/3} \left(\phi_\varepsilon^{n+s}\right)^{1/3} u_*} \right\} \tag{50}$$

where $\overline{-L}/z_i$ is an average stability parameter for the convective PBL, in which a typical value $\overline{-L}/z_i = 0.01$ will be used and $c_i = \alpha_i (0.5 \pm 0.05)(2\pi\kappa)^{-2/3}$ with $\kappa = 0.4$ and $\alpha_i = 1, 4/3, 4/3$ for u, v and w components, respectively (Sorbjan, 1989).

To construct the wind velocity variances and Lagrangian decorrelation time scales from equations (48), (49) and (50) for PBL Lagrangian dispersion models, it is necessary to have expressions for $w_*, u_*, \psi_\varepsilon, \phi_\varepsilon^{n+s}, (f_m^*)_i^c$ and $(f_m^*)_i^{n+s}$.

For a convective PBL, $(\psi_\varepsilon)^{2/3} \approx 0.75$ (Wilson, 1997), $w_* = (u_*)_0 (-z_i / \kappa L)^{1/3}$ and, recalling that $(f_m^*)_i^c = z/(\lambda_m)_i$ and that $(\lambda_m)_i$ is the peak wavelength of the turbulent velocity spectra, $(f_m^*)_i^c$ expressions for $i = u, v, w$ can be derived. According to Kaimal et al. (1976), Caughey (1982) and Degrazia and Anfossi, (1998)

$$(\lambda_m)_u = (\lambda_m)_v = 1.5 z_i \text{ and } (\lambda_m)_w = 1.8 z_i \left[1 - \exp\left(-4\frac{z}{z_i}\right) - 0.0003 \exp\left(8\frac{z}{z_i}\right)\right] \tag{51}$$

so that

$$\left(f_m^*\right)_i^c = z/\left(B_i z_i\right) \tag{52}$$

$$\text{with } B_u = B_v = 1.5 \text{ and } B_w = 1.8\left[1 - \exp\left(-\frac{4z}{z_i}\right) - 0.0003\exp\left(\frac{8z}{z_i}\right)\right] \tag{53}$$

For a neutral or stable PBL ϕ_ε^{n+s} can be written (Sorbjan, 1989) as $\phi_\varepsilon^{n+s} = \phi_\varepsilon^n\ (1+3.7z/\Lambda)$, where $\phi_\varepsilon^n = 1.25$ and $\Lambda = L(1-z/h)^{(1.5\alpha_1-\alpha_2)}$ is the local Monin-Obukhov length. For a shear dominated stable boundary layer, $\alpha_1 = 1.5$ and $\alpha_2 = 1.0$. Furthermore, for a neutral or stable PBL, $u_*^2 = (u_*^2)_0(1-z/h)^{\alpha_1}$ in which $\alpha_1 = 1.7$ for the neutral case (Wyngaard et al., 1974). Then, following Stull (1988) and Sorbjan (1989), and by considering $(u_*)_0 / G = 0.03$ (Hanna, 1982) follows that:

$$\left(f_m^*\right)_i^{n+s} = \left(f_m\right)_{is}^n\left(1 + 0.03a_i\frac{f_c z}{\left(u_*\right)_0} + 3.7\frac{z}{\Lambda}\right) \tag{54}$$

where $(f_m)_{is}^n$ is the frequency of the spectral peak in the surface for neutral conditions, G is the geostrophic wind speed and $f_c = 10^{-4}\,s^{-1}$ is the Coriolis parameter. According to Sorbjan (1989), $(f_m)_{us}^n = 0.045$, $(f_m)_{vs}^n = 0.16$ and $(f_m)_{ws}^n = 0.33$. Furthermore, $a_w = 500$ (Hanna, 1968; Hanna, 1981); as a consequence of the Blackadar mixing length hypothesis (i.e., the asymptotic length scale $l_\infty \approx G/f_c$ is limited by a constant value, equal for all the components) we found $a_u = 3889$ and $a_v = 1094$.

2.4.3 Formulas for $\overline{w^3}$ in the CBL

In a CBL with non-divergent horizontal flow, the vertical velocity has a zero mean value but a strongly negative mode (the most frequent value of the vertical velocity). This indicates that within the CBL (except in shallow layers near the ground and in the capping inversion base), the probability density of the vertical velocity fluctuations has a positive skewness. In the present subsection we present four expressions for the vertical profile of the third moment of the vertical velocity in a CBL, suggested by Rotach et al. (1996), Weil (1990), Luhar and Britter (1989) and De Baas et al. (1986), respectively. These formulations for the third moment of the vertical wind velocity fluctuations are the following:

i) Rotach et al. (1996)

$$\frac{\overline{w^3}}{w_*^3} = 1.3\left(\frac{z}{z_i}\right)\left(1-\frac{z}{z_i}\right)^2 \tag{55}$$

ii) De Baas et al. (1986)

$$\frac{\overline{w^3}}{w_*^3} = 1.4\left(\frac{z}{z_i}\right)\exp\left(-2.5\frac{z}{z_i}\right) \tag{56}$$

iii) Luhar and Britter (1989)

$$\frac{\overline{w^3}}{w_*^3} = 0.8\left(\frac{\overline{w^2}}{w_*^2}\right)^{3/2} \tag{57}$$

iv) Weil (1990)

$$\frac{\overline{w^3}}{w_*^3} = 0.84\left(\frac{z}{z_i}\right)\left(1-\frac{z}{z_i}\right) \tag{58}$$

2.4.4 Formulas for ε

Many expressions for the dissipation rate ε can be found in the literature. Among them the following are reported.

In convective conditions (Weil, 1994):

$$\frac{\varepsilon z_i}{w_*^3} = 0.85 - 1.25\frac{z}{z} \qquad \frac{z}{z_i} < 0.4 \tag{59}$$

$$\frac{\varepsilon z_i}{w_*^3} = 0.49 - 0.36\frac{z}{z} \qquad \frac{z}{z_i} \geq 0.4 \tag{60}$$

In stable conditions, PBL is generally rather shallow and consequently can be modelled with near surface layer scaling (Kerschgens et al., 2000). According to Kaimal and Finnigan (1994) ε can be estimated by

$$\varepsilon = \frac{u_*^3}{\kappa z}\left(1+5\frac{z}{L}\right) \tag{61}$$

Alternatively, ε can be obtained by equation (13).

2.4.5 Additional Parameterisations

One problem with the use of LSMs for real situations is that the technique is computationally expensive, although this is becoming less of a problem with the availability of faster computers. This problem was overcome to a large extent by Hurley and Physick (1993a, b), by using a homogeneous, skewed form of the Langevin equation and associated turbulence parameterisations,

$$\sigma_{u,v,w} = 0.6 w_{*,} \qquad T_{Lu,Lv,Lw} = 0.6 z_i / w_* \tag{62}$$

that agrees with observations in the middle 80% of the CBL. This approach reduced the number of terms to be calculated in the Langevin equation and enabled a much larger timestep to be used. By comparing results to the Willis and Deardorff (1976, 1978, 1980, 1983, 1987) and Deardorff and Willis (1982) experiments, they showed this simplified model could reproduce the important aspects of the experiments for CBL dispersion, and plume rise and entrapment, while decreasing the computational expense by an order of magnitude.

More recently, Nasstrom and Ermak (1999a, b) developed a model for dispersion in skewed homogeneous turbulent flow using a form of the Langevin equation that has a linear (in velocity) deterministic acceleration term and a non-Gaussian process for the random acceleration term. This model contrasts with that of Hurley and Physick, which incorporated, a non-linear deterministic term and a Gaussian random term, following the findings of Thomson (1987). Although both models are able to accurately simulate the (w,z) phase space trajectory of a particle, the advantage of the Nasstrom and Ermak model is that it is able to use a time step that is four times larger than that of the non-linear-Gaussian model.

The problem of reducing the computer time, maintaining the physical correctness (i.e., the well mixed condition) was also dealt with by Tinarelli et al. (2000), who adopted a variable time step Δt. For a correct numerical integration of the Langevin equations, the time step must be a small fraction of the smaller Lagrangian time scales (τ_x, τ_y, τ_z). The latter attain small values near the boundaries of ABL and much larger values in the main part of the ABL. Thus using a constant, and therefore very small, time step leads to unnecessarily long computer times. Following a suggestion of Wilson and Flesch (1993), these authors introduced three "vertical inhomogeneity time scales" defined as follows:

$$\tau_f(x,y,z) = \left(\frac{\sigma_w}{f} \frac{\partial f}{\partial z} \right)^{-1} \tag{63}$$

where *f*, in turn, is $\overline{w^2}$, $\overline{w^3}$ and the three Lagrangian time scales τ_i, and chose Δt as a small fraction $(1/5, 1/10)$ of the minimum time scale among τ_x, τ_y, τ_z and the three τ_f 's.

In the following Section, the wider range of turbulence parameterisations available to an LSM when linked to a meteorological model is discussed.

2.5 Link with Meteorological Models (W.L. Physick, S. Trini Castelli)

To assess the physics of transport and diffusion of pollutants, it is necessary to provide a description of the meteorological processes in the atmosphere, where the main parameters associated with dispersion problems are the mean wind field, turbulence, surface-layer parameters and the height of the atmospheric boundary layer. In the case of LSMs, the mean wind transport of marked particles can be derived from observations or from diagnostic and prognostic meteorological models. The turbulence fields for the diffusion can be obtained by combining similarity theory with empirical parameterizations (Section 5) or can be transferred directly from a meteorological model, when that model's turbulence is predicted using a turbulent kinetic energy scheme.

In section 3, it was shown that the correct general form of the Langevin equation is

$$dw' = a dt + (C_0 \varepsilon)^{0.5} dW \tag{64}$$

where a_i is a function of moments of the turbulent velocity distribution and ε is the eddy dissipation rate. In Gaussian turbulence, only the second-order moment (the variance) is needed, whereas for non-Gaussian turbulence (e.g. convective boundary layer turbulence) the third and sometimes fourth-order moments must be specified (see Section 4). Here we discuss how these variables are obtained when a LSM is linked to a meteorological model.

When a *diagnostic* wind model (discussed in Chapter 5) or wind observations provide the meteorology for a LSM, the mean winds are used to transport particles, but the necessary turbulence parameters (dissipation rate and moments) must be specified in the LSM using formulations such as those discussed in Section 5. These schemes are written in terms of Lagrangian de-correlation timescale T_{Li} rather than the eddy dissipation rate, but for the vertical component, the two variables are often linked via the relation

$$T_{Lw} = \frac{2\sigma_w^2}{C_0 \varepsilon} \tag{65}$$

(see equation 13). Meteorological parameters needed by formulations such as those of Hanna and Degrazia et al. in the previous Section include z_i, L, w_*, z_0,

and u_*. These are difficult to estimate if only wind data are available, but methods such as those proposed by van Ulden and Holtslag (1985) can be used to estimate these parameters from routinely available meteorological measurements.

When the winds from a *prognostic* meteorological model are used to drive a LSM, then a meteorological pre-processor prepares these parameter values from the output of the prognostic model. In this way there is consistency between the winds and turbulence parameters used in the LSM. For example, in the RMS modeling system, the meteorological model RAMS (Pielke et al., 1992) and the Lagrangian stochastic particle model SPRAY (Tinarelli et al., 1994, Tinarelli et al., 2000) interface through the pre-processing code MIRS (Trini Castelli and Anfossi, 1997, Trini Castelli, 2000). MIRS processes the meteorological fields produced by RAMS (or alternatively, data fields derived from observations or diagnostic models) and prepares the meteorological file as input to SPRAY.

Pre-processors can offer a number of options to calculate the atmospheric boundary layer parameters, especially the height of the boundary layer. Several approaches for estimating the latter in convective conditions are proposed in the literature. For instance, MIRS includes the Gryning and Batchvarova (1990) simplified model and its complete version, Batchvarova and Gryning (1991), the gradient Richardson number profile method, where the ABL inversion layer is identified by the height where Ri overtakes a critical value Ri_c (Maryon and Buckland, 1994, McNider and Pielke, 1981), and the diffusion coefficient profile method. The latter detects the inversion layer height by considering discontinuities in the diffusion coefficient profile and is limited to diurnal simulation. In particular meteorological conditions a constant ABL height can sometimes be assumed over the entire domain (e.g. Kalthoff et al., 1998). The Deardoff (1974) boundary layer height is often employed for neutral conditions while the stable boundary layer height is usually estimated by the Zilitinkevich (1972) formulation. Estimation of a boundary – layer height in stable conditions is often difficult, and this can be avoided by using an expression for σ_w involving the local Richardson number (McNider et al. 1988).

However a value for z_i is only needed when schemes such as those of Hanna or Degrazia et al. are employed in a LSM to describe the turbulence, or to define the upper boundary of the diffusive volume, permeable or impermeable, in the LSM. When a prognostic meteorological model with a turbulent kinetic energy (TKE) boundary-layer scheme provides the fields for a LSM, the dissipation rate and moments needed by equation (64) can be calculated from the meteorological model's TKE fields. Using TKE profiles avoids further parameterisation (meaning 'simplification') of the ABL structure, although some TKE schemes do not predict ε, necessitating a parameterisation in terms of the TKE. A disadvantage can occur at nighttime when TKE values, and hence variances, can be so low that an arbitrary lower limit needs to be set in order to simulate realistic diffusion. An evaluation of ten TKE schemes, including tracer experiments was carried out by Hurley (1997), while examples of coupled meteorological and Lagrangian stochastic models using TKE boundary-layer formulations can be

found in Yamada (1985), Tremback et al. (1993), Uliasz (1994), Hurley (1999) and Ferrero et al. (2000a). The latter two use third and fourth-order moments for the convective boundary layer.

Two different approaches to interface the meteorological and the dispersion model are used; '*online*' when the particle model is run at the same time as the meteorological model, and '*offline*', when the particle model is run from the stored output (usually at hourly intervals) of a meteorological simulation carried out previously. The *online* approach has the advantage of proposing an integrated modelling system and of providing a contemporary run-time meteorological and dispersive scenario. In this way too, the dispersion model results are able to affect the meteorology (e.g. aerosol levels can affect radiation calculations). In the case of the *offline* approach, the advantage is the independence of the two models and the consequent flexibility, so that different configurations for the dispersion description can be set and tested without having to re-run the meteorology each time. A disadvantage of running a dispersion model offline is that it is possible to introduce large errors in the trajectories of particles in regions of rapidly–changing winds, such as coastal areas. The vast majority of air quality models, including those referred to in this section, are run in offline mode, apart from the model TAPM (Hurley 1999, Hurley et al. 2001) which uses an integrated approach that also allows for specification of the emissions as a function of the meteorology.

2.6 Boundary Conditions (W.L. Physick)

At the lateral and upper boundaries of a two- or three-dimensional LSM, particles are usually allowed to pass out of the modelling domain and are no longer tracked. However at the lower boundary, and in those models where the upper boundary is considered to be rigid (e.g. a model of the convective boundary layer (CBL)), a condition is needed for a particle impinging on a boundary. A more complex condition is necessary when deposition is being simulated and particles are specified to lose a fraction of their mass at the rigid boundaries (see section 13.4). A further situation addressed in this sub-section is the correct formulation to allow exchange of particles across an interface with a discontinuity in turbulence properties.

2.6.1 Upper and Lower Boundary Conditions

The mathematical boundary condition on turbulent vertical velocity that is commonly applied at the upper and lower boundaries of an LSM, is that of perfect reflection, i.e. a particle impinging on a boundary leaves the boundary in the opposite direction but at the same speed. This condition is appropriate for Gaussian turbulence or skewed inhomogeneous turbulence (where the Lagrangian time scale is normally very small near the boundaries), but if used for skewed homogeneous turbulence will lead to an accumulation or deficit of particles at the boundaries. Modifications of the perfect reflection condition for non-zero skewness by Weil (1990) and Hurley and Physick (1993a) were shown by

Thomson and Montgomery (1994) (TM) to provide acceptable solutions for small values of the Lagrangian time-scale τ, but the departure from a uniformly-mixed profile became greater as τ increased. Considering now only the lower boundary, TM proposed that a correct boundary condition is

$$\int_{w_r}^{\infty} wP_E(w, z_b)dw = \int_{-\infty}^{w_i} wP_E(w, z_b)dw \tag{66}$$

where w_r is the reflected velocity, w_i is the incident velocity and P_E is the assumed vertical velocity distribution of particles at the boundary z_b (a corresponding equation can be derived for the upper boundary). The basis of this equation was their assertion that the relevant quantity to be considered is the PDF of the velocities of particles which leave z_b during a fixed time interval, rather than just the PDF of particles leaving the boundary at a particular time t, $P_E(w, z_b) / \int_0^{\infty} P_E(w, z_b)dw$ ($w \geq 0$), as used by Weil (1990). The former PDF is $wP_E(w, z_b) / \int_0^{\infty} wP_E(w, z_b)dw$ ($w \geq 0$) since more of the faster-moving particles will leave $z = z_b$ in a given time interval.

Knowing the incident velocity w_i of a particle, equation (66) is used to obtain w_r. When P_E is the commonly-used bi-Gaussian expression for skewed convective turbulence (equations 16 and 17**),** the solution to equation (66) consists of numerical integrals and error functions and is obtained for each particle from prepared look-up tables (TM). The time-consuming nature of this process in a three-dimensional Lagrangian stochastic model has been addressed by Anfossi et al. (1997) who proposed two approximate analytical solutions to equation (66). The first one made use of a Taylor series expansion and still involved error functions, but the second one involved a regression curve between w_i and w_r as a function of skewness and $w_i / \left(\overline{w}^2\right)^{1/2}$. Curve coefficients were obtained from many "exact" (look-up table) solutions to equation (66) over a range of variance and skewness values. Although both solutions of Anfossi et al. satisfy the well-mixed condition and do not appreciably depart from the correct or "exact" solution, the regression method uses considerably less computing resources and seems a suitable approach to applying boundary conditions in three-dimensional particle models. Note that although Anfossi et al. used the Baerentsen and Berkowicz (1984) closure (see section 4), their solutions can be modified for other closure schemes.

While the above formulation of the boundary condition is based on a positive correlation between the incident and reflected speeds, Nasstrom and Ermak (1999b) developed and tested a formulation in which reflected speed is negatively correlated with the incident speed. This originated from observation of near-surface convective circulation patterns in which air in the core of a downdraft region penetrates deep into the surface layer and, rather than moving back up

immediately, spreads away from its centre along the surface, while moving horizontally toward convergence zones that feed the updrafts in the mixed layer. Application of this boundary condition in simulations of the Willis and Deardorff (1976, 1978, 1981) convective tank experiments clearly showed its superiority over the positively-correlated condition.

2.6.2 An Interface Condition

The problem of random-walk modelling of diffusion across an infinitesimally-thin interface at which the turbulence statistics change discontinuously has been addressed by Thomson et al. (1997). They argued that if the Lagrangian time scale τ on which particles forget their velocity is much larger than the time particles spend within the interface, then particle trajectories in (*z*,*w*)-space within the interface are deterministic and do not cross each other. As a result, the trajectories will generally take the form illustrated in Figure 1(a), although cut-off circulations (Figure 1(b)) and other configurations are possible.

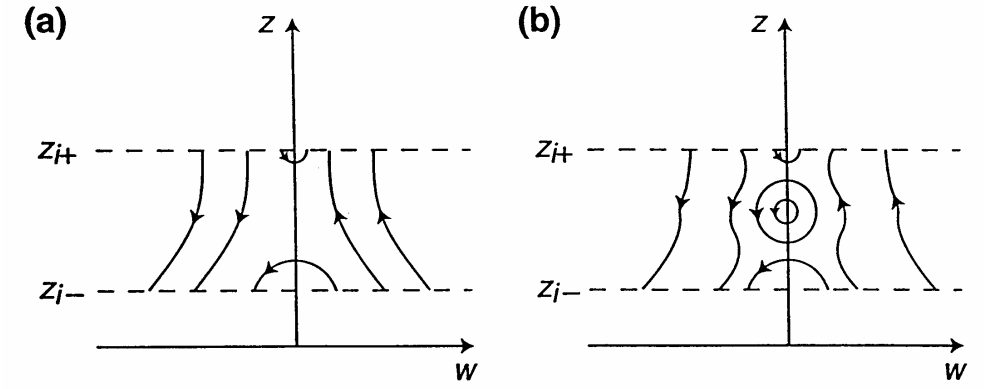

Figure 1. Illustration of some possible flows in (z,w)-space. From Thomson et al. (1997)

By using the fact that the flux between two streamlines in (*z*,*w*)-space must be conserved, and considering a particle entering the interface (lower and upper boundaries z_{i-} and z_{i+}) from below with incident velocity w_i, they show that its velocity *w* at a height *z* within the interface can be obtained from

$$\int_w^\infty w p_a(z,w)dw = \int_{w_i}^\infty w p_a(z_{i-},w)dw \qquad (67)$$

where p_a is the density of well-mixed tracer particles. Equation (67) is equally applicable if $w < 0$. From here on, the integrals will be denoted by *F*, e.g. the left-hand side of equation (67) is $F_w^\infty(z)$. If $F_0^\infty(z) < F_{w_i}^\infty(z_{i-})$ at any height in the interface then the particle will be reflected, i.e. the particle will be reflected if w_i is less than the critical value w_c which is defined for the CBL case of $F_0^\infty(z)$ decreasing monotonically within the interface by

$$F_{w_c}^{\infty}(z_{i-}) = F_0^{\infty}(z_{i+}) \tag{68}$$

Otherwise the particle will be transmitted. The reflection and transmission velocities w_r and w_t are given by

$$F_{w_r}^{\infty}(z_{i-}) = F_{w_i}^{\infty}(z_{i-}) \quad (w_r < 0) \tag{69}$$

and

$$F_{w_t}^{\infty}(z_{i+}) = F_{w_i}^{\infty}(z_{i-}) \quad (w_t > 0) \tag{70}$$

Similar relations can be derived for particles entering the interface from above. Note that particles approaching the interface from the side of weaker turbulence (above in the CBL case) are always transmitted. When implementing the interface condition in a random walk model, the particle velocity should be changed at the instant the particle reaches the interface, with z ($t+\Delta t$) being calculated in a way that accounts for the change in velocity during the time step.

2.7 Concentration Calculations Using Particle Models (W.L. Physick)

Particle models are a set of algorithms for the generation of realistic trajectories of imaginary, fictitious particles that simulate atmospheric motion. Each particle can be tagged by a mass of pollutant that can be either constant or time-varying to allow loss of mass due to ground deposition and chemical decay phenomena. If the emission rate of a pollutant is Q g s^{-1} and the release rate of particles is N s^{-1}, then the mass of each particle is Q/N g. In this way, the spatial distribution of particle mass in the computational domain allows the calculation of a three-dimensional mass concentration field, under certain computational assumptions.

For example, the most straightforward assumption is the superimposition in the computational domain of a three-dimensional concentration grid, with spacing (Δx, Δy, Δz). As one particle in the sampling domain represents a concentration of

$$C = Q/(N\Delta x\Delta y\Delta z), \tag{71}$$

the concentrations are computed simply by counting the number of particles in each grid cell and accumulating their masses. If concentrations need to be computed only at 'receptor' points (e.g. at a ground level), receptor cells can be defined around these points and particles counted only inside those cells. A rigorous concentration calculation, however, should not just add up the particle mass in a given cell at a given time. In fact, the contribution of each particle mass should be weighted by the total time the particle spent inside the cell during each time step (Lamb, 1979), although in reality this is rarely done.

It is important that sufficient particles are released per timestep to give meaningful concentrations. One way to address this problem is to calculate N according to the desired accuracy of the predicted ground-level concentrations. If this accuracy is denoted by e, then C must be less than e. This relation is used to calculate the minimum value of N in the following manner.

$$N = Q/(e\Delta x\Delta y\Delta z) \tag{72}$$

A three-dimensional mesoscale LSM is often run in two modes; *near-source* mode to determine the maximum GLC, which usually occurs within 5 km of a stack in convective conditions, and *far-field* mode to examine dispersion many kilometres from the stack. Experiments have shown (Physick et al., 1994b) that a sampling box of 1000 x 1000 x 25 m is adequate to calculate GLCs at distances further than 5 km from the source, but that it is necessary to reduce the box size to 250 x 250 x 25 m to obtain realistic GLCs closer in.

One of the great advantages of Monte-Carlo particle models, however, is their 'grid-free' characteristics, which allow higher time and space resolution than other simulation techniques. In this respect, grid-free concentration calculations (i.e. calculations that do not require the definition of cells) to maintain this important feature of the model are appealing. 'Kernel' methods (Gingold and Monaghan, 1982) allow grid-free concentration calculations that are smooth and efficient. Kernel methods for air quality modelling are discussed by Lorimer (1986). A general form of kernel density estimator is

$$c(\mathbf{r},t) = \frac{A(\mathbf{r})}{l^3}\sum_{i=1}^{n} m_i W(\mathbf{r}_i - \mathbf{r}, l) \tag{73}$$

where c is the concentration in $\mathbf{r}$ at time t; l is the time-dependent resolution bandwidth (or smoothing length); m_i is the pollutant mass of each particle i; W is the smoothing kernel, which is a function of l and the distance $\mathbf{r}_i - \mathbf{r}$ of each particle i from the receptor point. $A(\mathbf{r})$ is a correction term for concentration computations at locations $\mathbf{r}$ close to the boundary of the computational domain D, where

$$A(\mathbf{r}) = \frac{l^3}{\int_D W(\mathbf{r}' - \mathbf{r}, l)d\mathbf{r}'} \tag{74}$$

which, for an infinite domain D, reduces to $A(\mathbf{r})=1$ everywhere.

Several kernel functions W are available in the literature, and a discussion of the optimal choice of kernel for different situations is given by de Haan (1999). The most common is the Gaussian kernel, in which

$$\mathbf{d}_i = \mathbf{r}_i - \mathbf{r} \tag{75}$$

and

$$W(\mathbf{d}_i, l) = \frac{1}{(2\pi)^{3/2}} \exp\left(-\frac{1}{2} \frac{|\mathbf{d}_i|^2}{l^2} \right) \tag{76}$$

The choice of l is critical. This term should not be kept constant as is done in many applications, but should change in relation to a natural length scale. In general, l should be particle dependent and should be related to the mean interparticle separation around $\mathbf{r}$. Only particles with $|\mathbf{d}_i| < l$ give substantial contribution to c (Lorimer, 1986). If l is too small, the spatial distribution of the concentration c is 'jagged' with a series of local maxima at each $\mathbf{r}_i$; if l is too large, c becomes overly smooth.

Using a Gaussian kernel, the particle model becomes very similar to the puff models described in Chapter 8. It is important to note, however, that for a puff model, l is substituted by σ_x, σ_y, and σ_z (i.e., the standard deviations of the spatial concentration distributions of each puff), and these values are related to the physics of atmospheric diffusion, while, in the kernel method, l should be related only to the density of the particles around $\mathbf{r}$. However, Yamada and Bunker (1988) use a kernel density estimator, for their RAPTAD particle model, which makes it, in reality, a puff model, in which each particle i is associated with time-growing σ_{xi}, σ_{yi} and σ_{zi} values that are estimated based on the homogeneous diffusion theory by Taylor (1921).

2.8 Buoyancy Phenomena Simulation (H. van Dop)

The concept of the random walk has some attractive features also for plume rise formulations. Zannetti (1984) and Cogan (1985) (see Chapter 6) pioneered Lagrangian models for buoyant dispersion, however, on a somewhat ad-hoc basis. Also in section 6.4.4 a more fundamental formulation of buoyant tracers is presented.

Two major aspects distinguish buoyant and passive dispersion:

(i) buoyant fluid particles 'create' their own turbulent field in an environment with its own turbulent characteristics, and
(ii) the exchange processes between the plume particles and the (turbulent) environment is an essential element in the dynamics.

The buoyant plume is an envelope, which contains a mixture of ambient and (most of the) originally released, buoyant fluid. Some of the original buoyant fluid may be taken away from the plume and become so remote that it is no longer considered to be part of it. On the other hand the volume of the plume expands

due to turbulent intrusions of ambient air resulting in an increasing ambient fraction and consequently, a gradual loss of plume buoyancy.

A Lagrangian plume particle can be defined as a small entity, which possesses the mean characteristics (velocity, temperature) of the plume. Stochastic fluctuations, directly related to the turbulent intensity within the plume, determine the rate of growth of the plume width and are superimposed on the mean characteristics. Ultimately the plume (particle) dynamics must converge to the environmental dynamics. An important difference, however, between temperature and velocity is that for velocity changes (by pressure forces), no mass exchange is required, whereas (turbulent) temperature changes require the exchange of (particle) mass and environmental mass, thus in conflict with the (conventional) idea of Lagrangian particles moving with conserved properties in a turbulent flow.

In the section 6.4.4 we shall formulate the dynamic equations for such a particle. It should be noted that this concept, where a plume is thought to consist of a superposition of many independent trajectories of plume particles disregards all kinds of non-linear processes within the infrastructure of the plume. Their dynamical effects are thus ignored.

According to inertial sub-range theory we expect the following relationship between the temperature dissipation function, ε_θ, and the structure function, D_θ:

$$D_\theta \equiv \overline{\left[\Theta(t) - \Theta(t+\tau)\right]^2} = \varepsilon_\theta \, \tau$$

We further expect that the autocorrelation of Θ is exponential, and consequently, its spectrum behaves as ω^{-2}. This enables the dynamic description of temperature to be suitably formulated in a Lagrangian framework as a Langevin equation:

$$d\Theta = -\frac{\Theta - \Theta_a}{T_p} dt + \varepsilon_B^{1/2} \, d\omega_B(t),$$

since it guarantees the above properties. As we shall see in section 6.4.4 the Lagrangian formulation explains the basic features of plume motion in complex environments.

2.9 Reactive Chemistry (P. Hurley)

A theoretical approach to the inclusion of reactive chemistry in a Lagrangian framework has, as yet, not been dealt with in a satisfactory way. This is true of all Lagrangian approaches (Plume, Puff and Particle models). In LSMs, many independent particles are tracked, along with information on position and incremental mass of a pollutant. First-order reactions, where there is a single species, can be represented fairly simply in a Lagrangian approach, by exponentially decaying particle mass. Higher-order reactions, where there are

more than one species, cannot be handled by changing individual particle mass, because of the non-linear nature of the chemical reactions.

For atmospheric applications, a hybrid Lagrangian/Eulerian approach is, so far, the only way of incorporating chemical reactions into Lagrangian air pollution models. For example, in the model of Chock and Winkler (1994a,b), a Eulerian Grid Model (EGM) incorporating a 10 reaction photochemical scheme is solved for pollutant advection and diffusion using an LSM, while chemistry is solved for using an EGM. Similarly, in the Lagrangian Atmospheric Dispersion Model (LADM) of Physick et al. (1994b), the LSM was extended to incorporate a simple, semi-empirical photochemistry scheme called the Integrated Empirical Rate (IER) method. LADM used an LSM approach to solve for advection and diffusion, and a local Eulerian approach to solve for the chemistry. These hybrid approaches use a method to convert between particle mass and total concentration as follows. At each timestep, for each particle, summed particle mass in a volume (either fixed grid or moving local grid) is converted to total concentration for each species, and then the chemical reactions are performed in this volume to determine new concentrations. These new concentrations are then converted back to individual particle mass using a mass weighted approach that uses the change in concentration and the previous (before reaction) particle mass. This approach has the advantage that both advection and diffusion for each species is solved for using the LSM approach, which is more accurate for advection and better represents diffusion close to point sources compared to the Eulerian approach, but has the disadvantage that conversion of concentration to particle mass is computationally expensive.

An alternative hybrid approach is used in The Air Pollution Model (TAPM) of Hurley (1999). In TAPM, an EGM incorporating the Generic Reaction Set (GRS) photochemical scheme, optionally includes an LSM for user-selected point sources. The approach taken in this model is that the LSM solves advection and diffusion for pollutant species emitted from selected point sources without chemical transformation, and the EGM is run side-by-side to include advection and diffusion by non-LSM sources and to compute the chemical reactions using total concentration (LSM+EGM). This approach avoids the need to convert between particle mass and concentration for use in the chemical reactions, thus saving computer resources. Note that this approach can allow the EGM concentration to be negative. For example, in the case when all emissions are represented by the LSM, then losses resulting from chemical reactions can result in negative concentration in the EGM, but positive total (LSM+EGM) concentration.

Of course, a preferred approach would be to include chemical reactions directly in the Lagrangian framework, but from a theoretical viewpoint it is not clear how this can be achieved at the moment.

2.10 Predicting Higher-Order Concentration Moments (A. Luhar)

One-particle Lagrangian stochastic models have been successful in capturing the essential features of mean tracer dispersion in the atmospheric boundary layer, and are now used routinely in larger-scale modelling systems for air quality management and impact assessment studies. However, since these models assume that each tracer particle has an independent motion, they can only predict the ensemble-mean concentration field. They cannot provide any information about the higher order concentration fluctuation statistics (e.g., the variance), which is required when addressing topics such as 'peak-to-mean' concentration ratios, odour estimates, uncertainty in air quality models, and accidental release of toxic and flammable gases.

The two-particle Lagrangian stochastic approach (see also Section 3), in which two particles are released simultaneously with their motions correlated, can provide information on the variance of the concentration distribution, but developments in this area have so far been restricted to (idealised) homogeneous, isotropic turbulence in studies of the fundamental aspects of relative diffusion (e.g., Thomson, 1990; Borgas and Sawford, 1994). An extension of this approach to inhomogeneous flows in the atmospheric boundary layer is difficult, largely because of the mathematical complexities generated by the turbulence characteristics, and the extensive input requirements (e.g., the field of two-point Eulerian velocity statistics) which, at present, can only be obtained from high-resolution turbulence models.

Recently, one-particle Lagrangian models have been used in conjunction with the meandering plume approach of Gifford (1959) to determine higher order concentration fluctuation statistics for practical applications (Weil, 1994; de Haan and Rotach, 1998; Luhar et al., 2000). The original analytical model of Gifford assumes that the total (or absolute) dispersion can be split into two independent (Gaussian) parts–the meandering part and the relative-diffusion part–with the production of the fluctuations caused solely by the meandering of the ensemble-mean instantaneous plume. The spread of the mean instantaneous plume is prescribed according to the relative diffusion theory. This model has been particularly successful for predictions close to the source where meandering is the primary mechanism responsible for generating fluctuations, but it ignores the in-plume fluctuations that dominate the overall fluctuation statistics in the far field.

In the skewed meandering plume model of Luhar et al. (2000), developed for the convective boundary layer, the relative diffusion is parameterised, and a one-particle Lagrangian model is used to determine the meander trajectory distribution of the instantaneous plume. The in-plume fluctuations in the model are accounted for via a gamma probability density function (PDF) based on the work of Yee and Wilson (2000). The use of the one-particle Lagrangian approach for the meander trajectory calculation accounts for the flow inhomogeneity. The model of Luhar et al. (2000) is an improvement over other models based on the meandering plume

concept (Weil, 1994; de Haan and Rotach, 1998), and can be applied to skewed as well as Gaussian turbulent flows.

In the meandering plume approach, the movement of the centroid of the instantaneous plume is described in a fixed (or absolute) coordinate system relative to the source while the concentration distribution within the instantaneous plume is specified in a relative (or local) coordinate system whose origin is located at the centroid of the instantaneous plume. All model concentration statistics are calculated in the fixed coordinate system. If one assumes that the plume meander in the lateral (i.e. crosswind) direction (y) is statistically independent of that in the vertical direction (z), the nth moment of concentration at location (y,z) at travel time t is given as (Luhar et al., 2000):

$$\overline{c^n}(t,y,z) = \frac{1}{\lambda^n}\frac{\Gamma(n+\lambda)}{\Gamma(\lambda)}\frac{1}{(\sqrt{2\pi}\sigma_{yr})^n}\frac{\sigma_{yr}}{(n\sigma_{ym}^2+\sigma_{yr}^2)^{1/2}}$$
$$\times \exp\left[-\frac{n\,y^2}{2(n\sigma_{ym}^2+\sigma_{yr}^2)}\right]\int_0^h(\bar{c}_{zr})^n(z,z_m,t)\,p_{zm}(z_m,t)\,dz_m$$

where $\lambda = 1/i_{cr}^2$, i_{cr} is the concentration fluctuation intensity in the relative coordinate system, $\Gamma(\lambda)$ is the gamma function, σ_{yr} and σ_{ym} are the relative and meander spreads, respectively, in the lateral direction, h is the boundary-layer height, $\bar{c}_{zr}$ is the mean vertical concentration distribution in the relative frame (which is taken to be skewed in the CBL), p_{zm} is the meander PDF in the vertical which is calculated numerically using a one-particle Lagrangian model. The above equation assumes that the lateral meander and relative components are Gaussian. It reduces to the concentration moment equation of Yee and Wilson (2000) if the vertical components are also assumed to be Gaussian, and further to Gifford's moment equation if the in-plume fluctuations within the relative plume are neglected (i.e., $i_{cr}\rightarrow 0$, $\lambda\rightarrow\infty$).

An animation of the output of the above skewed meandering plume model can be viewed at http://www.dar.csiro.au/res/aq/Meander/index.html.

3 LSM Applications

3.1 Simulation of Dispersion in Convective Conditions, Including Fumigation (P. Hurley)

LSMs have been used to model dispersion from passive point sources in both fully developed convective boundary layers (CBLs) and for fumigation into growing CBLs, including thermal internal boundary layers (TIBLs). Results from these models have been compared to data, including laboratory experiments relevant to the CBL, laboratory experiments of fumigation and CBL entrainment,

and field experiments. The demonstrated ability of LSMs to model both near- and far-source GLCs associated with emissions from elevated sources, especially in convective conditions, has led to them being applied to assessments of the impact of existing and proposed power stations, smelters etc. (Noonan et al. 1994; Physick et al. 1995).

Early applications of the LSM approach within a mesoscale meteorological model (e.g. McNider, 1981), suffered from the lack of a theoretical basis for the Langevin equation when applied to the inhomogeneous, skewed turbulence of the CBL (see also Section 2). Although simulations looked qualitatively reasonable, the Gaussian, homogeneous form of the traditional Langevin equation, even with the drift correction term of Legg and Raupach (1982), resulted in particle accumulation in regions of lower turbulence (e.g. near the boundaries of the CBL). The development of a form of the Langevin equation for Gaussian, inhomogeneous turbulence by Wilson et al. (1981) and Thomson (1984), allowed LSMs to be formulated in a way that alleviated this problem for Gaussian turbulence. Non-Gaussian or skewed turbulence, as present in the CBL, was usually included in LSMs through the random forcing term in the Langevin equation. For example, this approach was used by Baerentsen and Berkowicz (1984), De Baas et al. (1986) and Sawford and Guest (1987), and results from these models were compared to the laboratory experiments of Willis and Deardorff (1976, 1978, 1981). As described in Section 2.2, theoretical developments by Thomson (1987) allowed the use of a form of the Langevin equation that could handle skewed, inhomogeneous turbulence. This new theory allowed the skewed nature of the CBL to be more correctly incorporated into the non-random terms of the Langevin equation in a way that satisfied the well-mixed criteria, while leaving the random terms Gaussian. It was applied to model the laboratory experiments of Willis and Deardorff (1976, 1978, 1981) independently by Sawford (personal communication, 1989) and Luhar and Britter (1989).

Various closure schemes for PDFs under CBL conditions were discussed in Section 4.2, but the evaluation by Luhar et al. (1996) identified important differences between the schemes, with implications for modelling fumigation. The largest differences between closures occurred for the case where the source height was near the top of the CBL (which is relevant to fumigation). It is not only the peak ground level concentration value that is strongly influenced by the choice of closure scheme, but also the distance downwind at which the plume first reaches the ground. For this source height, the laboratory data against which the schemes were evaluated showed no distinguishable peak, a characteristic that was reproduced by two of the four closures, and was also observed for low entrainment rates in direct measurements of fumigation in further tank experiments by Hibberd and Luhar (1996). These laboratory fumigation experiments were designed to determine the influence of entrainment rate on concentration levels for a wider range of growth rates than previously examined by Deardorff and Willis (1982).

Comparison of LSM predictions to CBL and fumigation field data include those of Brusasca et al. (1989) for Karlsruhe, Rotach et al. (1996) for Copenhagen,

Ferrero et al. (1995) for Copenhagen, and Luhar and Sawford (1995) for Nanticoke. Generally, simulations compared well to data, and to predictions from simpler models. LSMs should also be compared to datasets gathered in convective conditions in complex terrain, as this is potentially where they will have advantages over Gaussian plume or puff Lagrangian models, as discussed in Section 3.5. More comparisons with field data are needed, and should be done with LSMs for the above-mentioned datasets, as well as for other available CBL datasets such as CONDORS (Eberhard et al., 1988) and Kincaid (Hanna and Paine, 1989) for the CBL, and Kwinana for coastal fumigation (Sawford et al.,1998).

3.2 Simulation of Dispersion in Stable Conditions (E. Ferrero)

As an example of application of an LSM to a real case in stable conditions, simulation results from the Lillestrøm (Norway) experiment (Gronskei, 1990; Olesen, 1998) are presented. The data set includes the measurements of tracer released from a 36 m mast. The campaign took place in an almost flat, residential area during winter with the sun at very low angles above the horizon. The ground was snow-covered, the temperature was around minus 20ºC and rather strong stable conditions prevailed, with low or near calm wind conditions (Olesen 1995). The comparison is made in terms of crosswind integrated concentrations (CY) and arcwise maximum (ARCMAX/Q), normalised by the emission rate Q, and the standard deviation of the crosswind concentration distribution (SIGY).

The Lillestrøm experiment was simulated with LSMs by Ferrero et al. (1996), Ries et al. (1997) and Rotach (1998). Ferrero et al. (1996) used, as input for the model, the measured data and the Hanna (1982) turbulence parameterisation (Section 5); for the horizontal Lagrangian time scales they imposed a constant value equal to 300 s and the boundary layer height was computed from: $z_i = 0.25\frac{u_*}{f}$. The results were satisfactory as far as SIGY is concerned, while the results about ARCMAX/Q and CY/Q were less accurate. It was also found that the model underestimates the concentrations on the first arc in some runs.

Ries et al. (1997) applied three LMSs to simulate the Lillestrom data set. Each model was initialized with the same pre-processor and wind standard deviations but with different Lagrangian time scale parameterisations. Despite this being the only difference, simulation results were significantly different, confirming the great importance of a correct choice of the time scales in LSMs (Ferrero and Anfossi, 1998).

Rotach (2001) applied a Lagrangian particle dispersion model to this data set distinguishing the urban cases, in which the roughness sub-layer is considered, from non-urban cases in which it is neglected. He suggested that, in the urban atmosphere, the surface layer is not close to the ground, but it is superposed to the roughness sub-layer, whose extension is 3 h_b, where h_b is the average building

height. The results obtained are comparable with those of Ferrero et al. (1996) except for SIGY, which is much less accurately predicted.

It should be mentioned that the Lillestrøm data set has some problems when models based on similarity theory for the turbulence description are used (Gryning, 1999). However, this data set was here introduced because, at our knowledge, there are no other published examples of LSM simulation of dispersion exercises carried out in stable conditions

3.3 Simulation of Dispersion in Neutral Conditions (E. Ferrero)

A useful representation of the real atmospheric flow in neutral conditions can be obtained in a wind tunnel. The initial and boundary conditions in the experiments carried out in such a facility can be controlled and accurately reproduced. For these reasons, these kinds of experiments are good tests for model evaluation. An example is the wind tunnel EPA-RUSVAL tracer experiment (Khurshudyan et al. 1990) which involved a neutral flow on a 2-D valley with an aspect ratio $a/H = 8$. Measurements were taken of the turbulence parameters and the 3D concentration field. (Ferrero et al. 1999) simulated this experiment using a complete 3-D model system (RMS, see also Section 2.5) based on the mesoscale model RAMS (Pielke et al.) the interface code MIRS (Trini Castelli & Anfossi, 1997, Trini Castelli, 2000) and the LSM SPRAY (Tinarelli et al. 2000). The simulated cases consisted of a source placed near the bottom of the valley. They implemented in RAMS two new turbulence models (E-l and E-ε), providing, through the code MIRS, the input for the dispersion model SPRAY. They found an improvement in the model results using the turbulent quantities directly calculated from the output of the turbulence model instead of using the Hanna (1982) parameterisations based on the surface layer theory.

In a previous work (Tinarelli et al. 1994) the same team applied an old version of SPRAY to a similar experiment carried out in the same wind tunnel (Khurshudyan et al., 1981) simulating a neutral flow over a gentle hill. The three-dimensional mean flow field was provided by a mass-consistent model and the turbulence quantities were parameterised. The results were satisfactory.

The validation of an LSM coupled to a mass-consistent model against data measured in a wind tunnel, was presented by Duran et al. (1998). They simulated the dispersion of radionuclides released from a reactor building of two nuclear power plants, the first one over flat terrain and the second over hilly terrain. The turbulence characteristics were modified in order to take into account the wake region generated by the building.

3.4 Simulation of Dispersion in Urban Conditions (E. Ferrero)

As an example of application of a LSM to a case of urban (stable and unstable) boundary layer the Indianapolis experiment (TRC, 1986) is presented. This data set includes many buoyant tracer releases in an urban area in different stability conditions. The emission point is an 84 m stack and measurements of ground level concentrations are available on arcs at distances between 0.25 and 12 km from the source. Meteorological data are given at different locations in urban, suburban and rural areas in the surface layer and some quantities have also been measured at a height of 94 m at the top of a building. Vertical profiles of wind velocity and temperature were gathered from minisondes and acoustic sounders. The model comparison is made in term of cross wind-integrated concentrations (CY), standard deviation of the crosswind concentration distribution (SIGY), arcwise maximum (ARCMAX) and azimuth of the maximum (AZMAX).

Both daytime and nighttime releases were simulated by Ferrero et al. (1998 and 1999), using a LSM. The input of the model was prescribed by both measured quantities and parameterisations (de Baas et al., 1986; Hanna, 1982) or similarity relationships. The model evaluation results for the daytime cases demonstrate that SIGY and AZMAX agree with the corresponding measured quantities while CY and ARCMAX are overestimated. In the simulations of the nighttime cases, the authors imposed a neutral parameterization in the case of $|L|>100$ (where L is the Monin-Obukhov length), in order to take into account the additional mixing due to the presence of the urban boundary layer, as also stressed by Hanna et al. (2001), obtaining better results than using stable parameterization.

The influence of a strong plume rise was stressed by Rotach (1998), who simulated the Indianapolis experiment with a LSM. He observed that plume rise reduces the effects of the roughness sub-layer concept introduced in his model and seems to be responsible for deficiencies in the simulations of the concentrations close to the source.

As another example, the Copenhagen tracer experiment can be considered. In particular, we refer to the following papers: Rotach and de Haan (1997), de Haan and Rotach (1998), Rotach (1999) and Rotach (2001). In Rotach and de Haan (1997), it is stressed that, in the urban boundary layer, a roughness sub-layer covers the lower part of the surface layer wherein surface layer scaling cannot be valid, owing to the presence of roughness elements and the resulting disturbances of the flow. If a roughness sub-layer is included by modifying the turbulence and flow structure in the lowest metres of the domain according to observed (urban) roughness sub-layer characteristics, it is shown that the model performance is considerably improved. In de Haan and Rotach (1998) the Copenhagen date set is used for validating the Puff-Particle Model, which is based on a particle model. All the statistics considered in the comparison show that this model is able to reproduce the tracer observations.

Satisfactory results in simulating these experiments were also obtained by Ferrero et al. 1995, using their LSM.

3.5 Simulation of Dispersion in Low Wind Speed Conditions (D. Anfossi)

Dispersion in low wind speed stable conditions is governed by meandering (low frequency horizontal wind oscillations), weak, layered and intermittent turbulence, air stagnation and gravity waves (Mahrt, 1999; Gryning, 1999). These characteristics give rise to highly non-stationary and inhomogeneous diffusion conditions. Even if the stability reduces the vertical dispersion, meandering disperses the plume over rather wide angular sectors. Thus, in particular, the resulting ground level concentration is generally much lower than that predicted by standard Gaussian plume models (Sagendorf and Dickson, 1974; Wilson et al., 1976). As a consequence, different types of models should be used. Among these, the LSM has proved to be a reliable modelling tool (see, for instance: Brusasca et al., 1992; Ries et al., 1996; Oettl et al., 2001).

Brusasca et al. (1992) proposed an "ad hoc" algorithm to account for the meandering in their LSM LAMBDA (Brusasca et al., 1989). This algorithm is based on the Gifford fluctuating plume model (1960). By defining σ_i (i = u,v) as the measured hourly averaged horizontal wind standard deviation, σ_i^T its part due to the turbulence and σ_i^M the remaining part due to the meandering σ_i^M, this last is computed as:

$$\sigma_v^M = \sqrt{\left(\sigma_v\right)^2 - \left(\sigma_v^T\right)^2} \tag{77}$$

The total sampling time (1 h) was split into N (= 20) sub-periods of 3-min. Then, series of wind vectors were randomly picked in such a way to obtain a close approximation of the observed hourly values of mean wind speed, mean wind direction and standard deviation. The model was tested against the Idaho National Engineering Laboratory (INEL) tracer data set (Sagendorf and Dickson, 1974). Three experiments, characterised by plume spread of 48º, 138º and 360º, respectively, at an arc of 200 m from the source, were chosen. The model reproduced the observed ground level concentrations with a reasonable degree of confidence.

Oettl et al. (2001), based their LSM on the analysis of the wind velocity Eulerian autocorrelation functions $R_i(\tau)$ computed over one year of sonic anemometer observations. The resulting $R_i(\tau)$ for the horizontal components of the wind vector showed a negative loop, attributed to the meandering. Their model uses a time-step PDF with uniform distribution (Wang and Stock, 1992). This means that random time-steps and a negative intercorrelation parameter $\rho_{u,v}$ for the horizontal wind components (to account for the observed $R_{u,v}(\tau)$ characteristics) are used. Mean time-interval $\overline{\Delta t_h}$ are calculated from:

$$\overline{\Delta t_h} = 3 \cdot T_{Lu,Lv} \cdot \left(\frac{1 - \rho_{u,v}}{2 + \rho_{u,v}} \right) \tag{78}$$

where $T_{Lu,Lv}$ are the Lagrangian decorrelation time scales and the PDF has the following expression:

$$f\left(\overline{\Delta t_h}\right) = \begin{cases} \dfrac{1}{2 \cdot \overline{\Delta t_h}} & for \quad \Delta t_h \le 2 \cdot \overline{\Delta t_h} \\ 0 & for \quad \Delta t_h > 2 \cdot \overline{\Delta t_h} \end{cases} \tag{79}$$

The result is an enhanced dispersion in low wind situations. Since the model reduces to the Langevin equation for $\rho_{u,v} = 0.9$, it can be used for all wind speeds simply by adjusting the intercorrelation parameter. This model was applied to the same INEL dispersion data (all the tests were simulated) and showed reasonable agreement.

3.6 Transport and Dispersion at the Mesoscale (W.L. Physick)

As well as showing skill in predicting near-source maximum GLCs from point sources, LSMs are particularly useful for applying to dispersion of pollutants by sea breezes and in complex terrain. It is not only the good agreement shown with observed concentrations that is impressive, but also the insight into the dispersion processes that is available through both static and animation plots of particle positions.

3.6.1 Sea Breeze Dispersion

Using a three-dimensional meteorological model (RAMS) and a LSM (LPDM), Lyons et al. (1995) discussed the importance for dispersion modelling of accounting for vertical motion. They showed that emissions from shoreline sources can be transported vertically out of the sea breeze inflow layer at the front, as illustrated in Figure 2, and back over the water at higher levels. Using the same models for the same region (Lake Michigan), Eastman et al. (1995) estimated that about 70% of emissions undergo at least one recirculation out over the lake and then back towards the shore. They also ran a Gaussian-plume model (ISC), which is unable to represent vertical motion or recirculation, and showed that surface concentrations derived from the two models differed significantly in structure and magnitude.

When offshore flow in coastal regions advects morning emissions out to sea, they are often returned in the sea breeze inflow during the afternoon. This different type of recirculation (in the horizontal plane) is the primary mechanism responsible for elevated ozone readings in all of Australia's major coastal cities.

A coupled meteorological and Lagrangian stochastic model (LADM) has been used successfully in these cities to understand the important processes involved (Physick, 1996). Similarly, recirculation of SO_2 has been observed and modelled with a LSM for Israel by Robinson et al. (1992).

Sea breezes are not just confined to near the coast, but can travel to at least 200 km inland. Buckley and Kurzeja (1997) observed that the sea breeze penetrates to the Savannah River Site (SRS, 150 km inland) from the eastern coast of U.S.A. on about 15% of all nights. Using RAMS and the stochastic model LPDM, Buckley and Kurzeja were able to investigate the sea-breeze dispersion of emissions from the SRS, concluding that vertical, horizontal and temporal wind shear, and vertical motion were the dominant factors in the plume dispersion. None of these effects are contained in the surface meteorological files used to run the simpler Gaussian models. In a study to investigate the effect of SO_2 emissions from coastal regions on National Park Service management areas in Southern Florida (80 km inland), Segal et al. (1988) used RAMS and LPDM, finding that the complexity of the dispersion patterns which can occur for such a large travel distance necessitate a realistic assessment of mesoscale dispersion in coastal regimes.

Kerr et al., (2001 a,b) applied the modelling system RMS (see Section 2.5) to investigate the effects of a typical breeze regime on dispersion in coastal complex terrain. The inhalable particulate matter emitted by Fertilizer Plants located at Cubatão (Brazil) was simulated. Cubatão is an industrial city placed on the flat terrain between the escarpment of *Serra do Mar* sierra (700 to 1000 m high) and the Atlantic Ocean. For a typical daytime circulation, the sea breeze may be blocked by the mountain escarpment (see Figure 3) or overcome the mountain ridge and penetrate deep inland (see Figure 4). Thus, on many occasions, the Cubatão emission may reach São Paulo (44 km inland). For a typical nighttime circulation, the katabatic winds and land breeze transport the particulate matter over the shoreline plains (see Figure 5) where many towns (700,000 inhabitants) are located

3.6.2 Dispersion in Complex Terrain

LSMs have been used in a number of simulations of the ASCOT (Atmospheric Studies in COmplex Terrain) tracer data sets. Luhar and Rao (1993) coupled their LSM to a 2D-katabatic flow model to simulate the tracer concentration data obtained over a nearly two-dimensional slope in the Anderson Creek Valley, California. Magnitude predictions were good at nearly all sampler sites, but observed concentrations decreased more slowly with time than the predicted ones, most likely due to pooling of the drainage air in the valley basin, causing flow stagnation and emphasising the need for a three-dimensional meteorological field, modelled or analysed.

Tracer concentrations from the 1991 ASCOT Colorado Front Range nocturnal experiment (near the Rocky Flats Plant) were modelled well with a LSM by Luhar and Rao (1994), using winds and turbulence parameters derived from analyses of the observed meteorological data. Their diagnostic approach can be compared to the prognostic approach of Poulos and Bossert (1995) and Fast (1995) who used three-dimensional meteorological models (Fast additionally used four-dimensional data assimilation) and LSMs to simulate the same period. The time- and space-varying nature of the drainage flow in this challenging region is illustrated by Figure 6 (from Fast, 1995), which shows the hourly-averaged concentration and streamlines at two different times. Fast (1995) compared his results, and those from Poulos and Bossert (1995), to the results from air quality models coupled to several diagnostic models and concluded that the latter predict more accurate maximum concentrations. He suggests that this may be due to the stable turbulence parameterisations in the mesoscale prognostic models (rather than the mean wind field) as these directly affect the way diffusion is treated in the LSMs.

Studies involving LSMs in complex terrain under daytime conditions include the Swiss Alps tracer experiments (Anfossi et al., 1998) and the evaluation of emissions from coastal power stations in Australia (Noonan et al., 1994) and Spain (Hernandez et al., 1995).

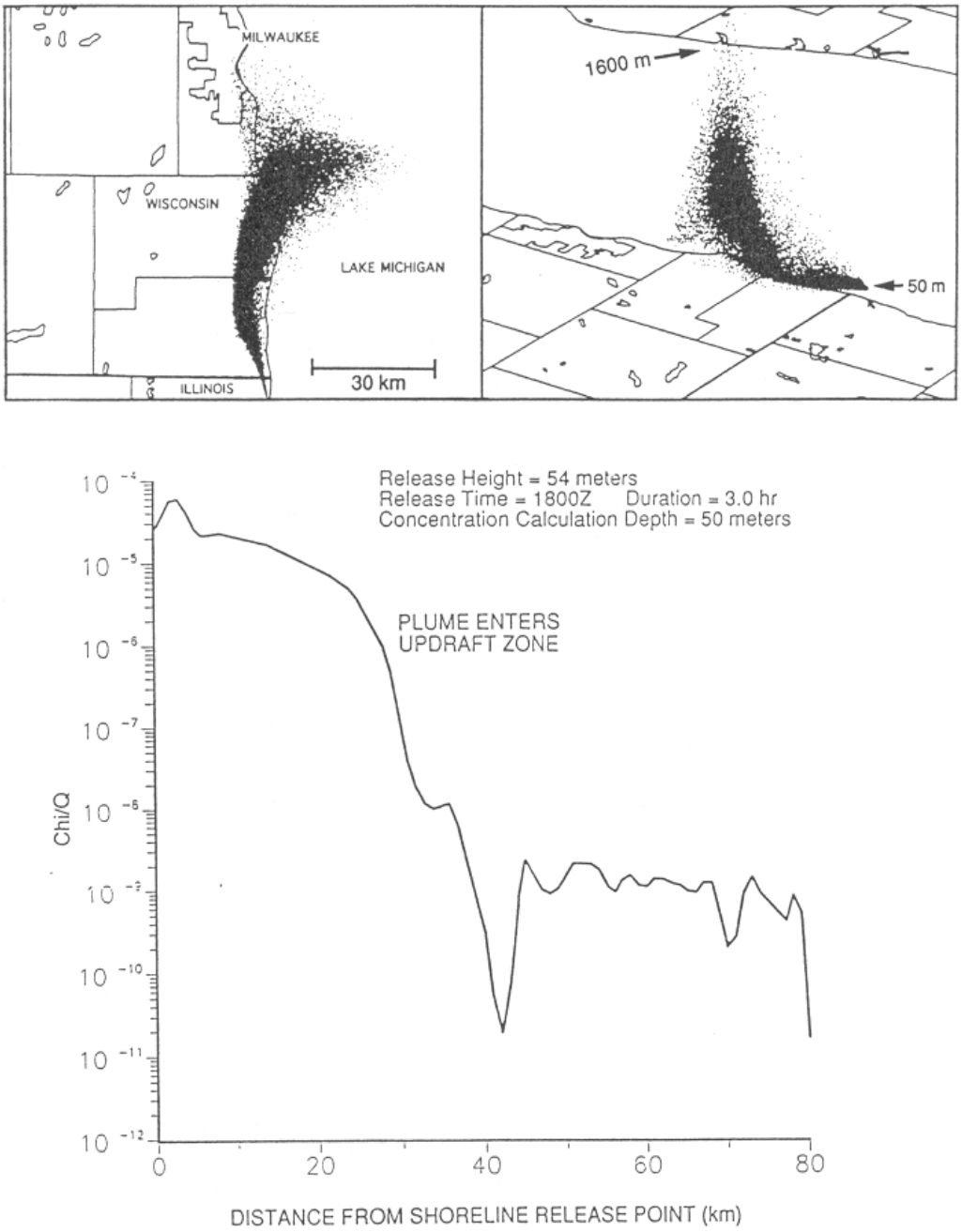

Figure 2. (a) (Top left). Plan view of a simulated plume released from a 50m high shoreline source into a weak lake breeze along the Lake Michigan shoreline. (b) (Top right) Perspective view of the plume from the southwest showing large quantities of the plume being translocated vertically as high as 1600 m due to the strong upward motions in the lake-breeze frontal zone. (c) (Bottom) Modelled normalised surface-layer concentrations at the centreline of the plume demonstrating a dramatic decrease as the plume intersects the lake breeze frontal updrafts.

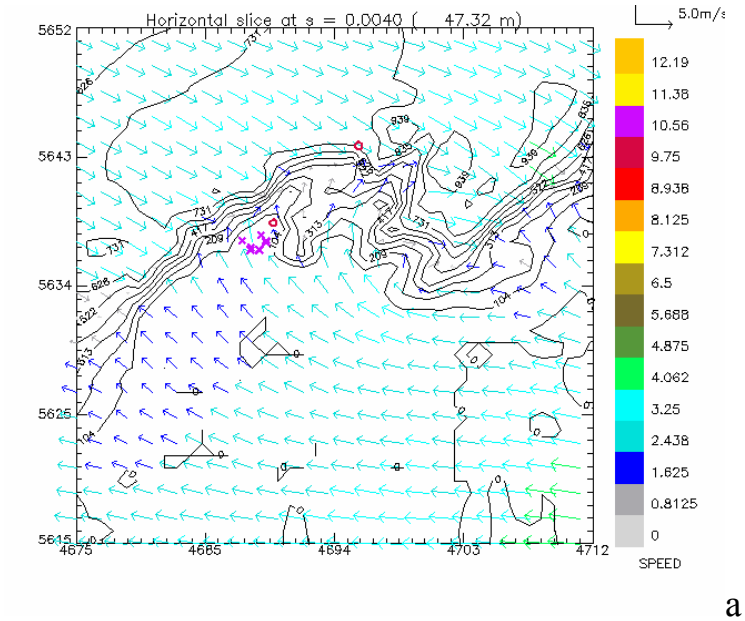

a

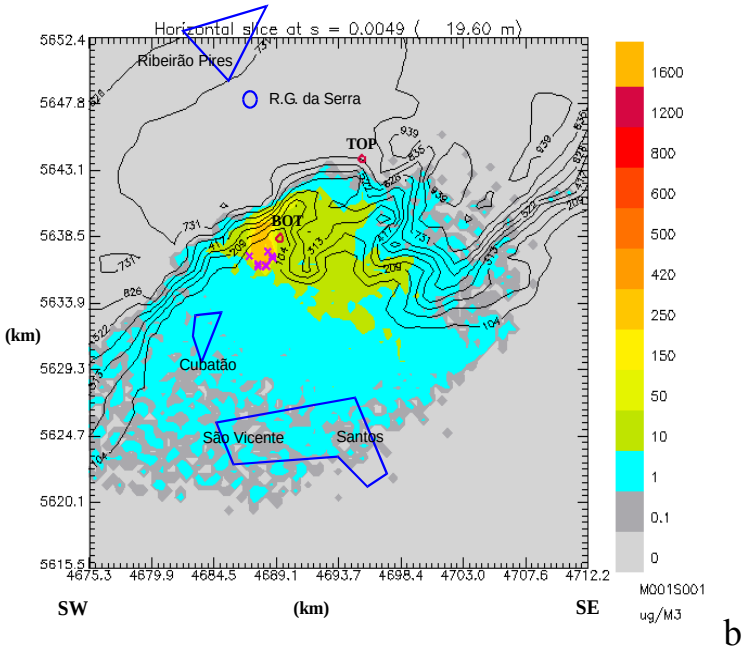

b

Figure 3. Typical daytime situation with blocked sea breeze. (a) wind field at 47 m a.g.l. computed by RAMS, the colour scale refers to the wind speed intensity in ms^{-1}; (b) concentration field at ground level, computed by SPRAY, the colour scale refers to concentration amounts in μgm^{-3}.

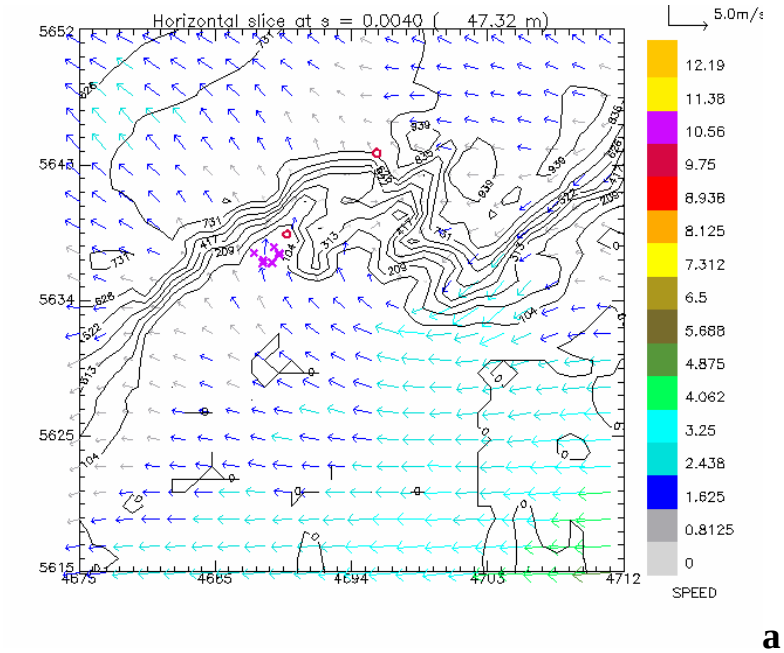

a

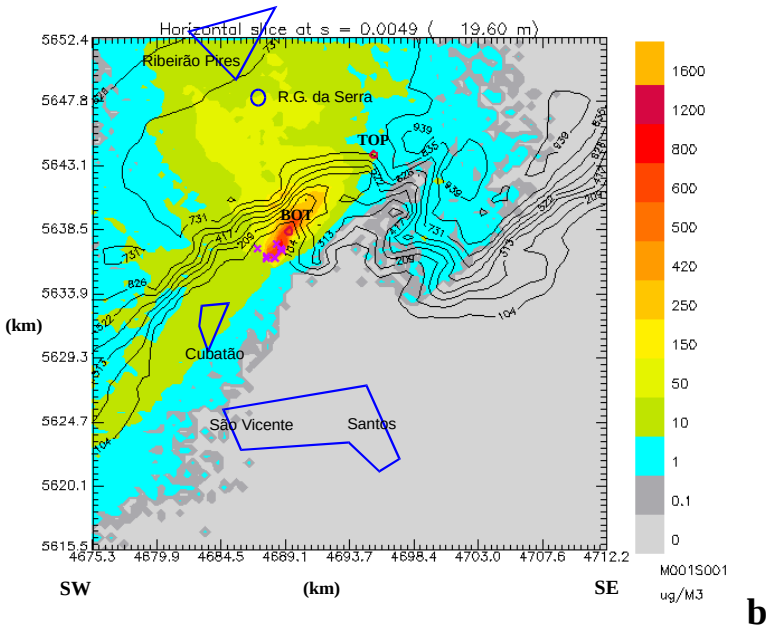

b

Figure 4. As in Figure 3 but for typical daytime situation with sea breeze overcoming the mountain barrier

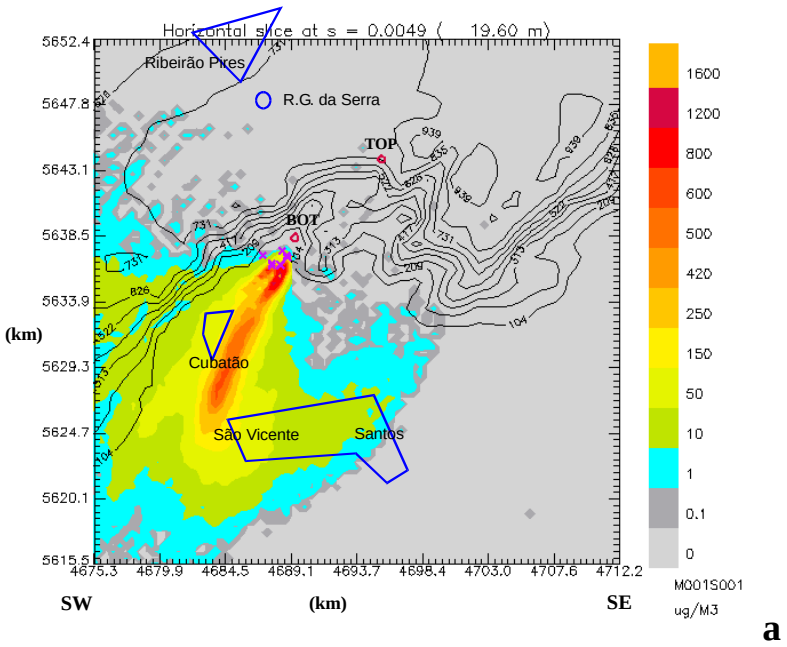

a

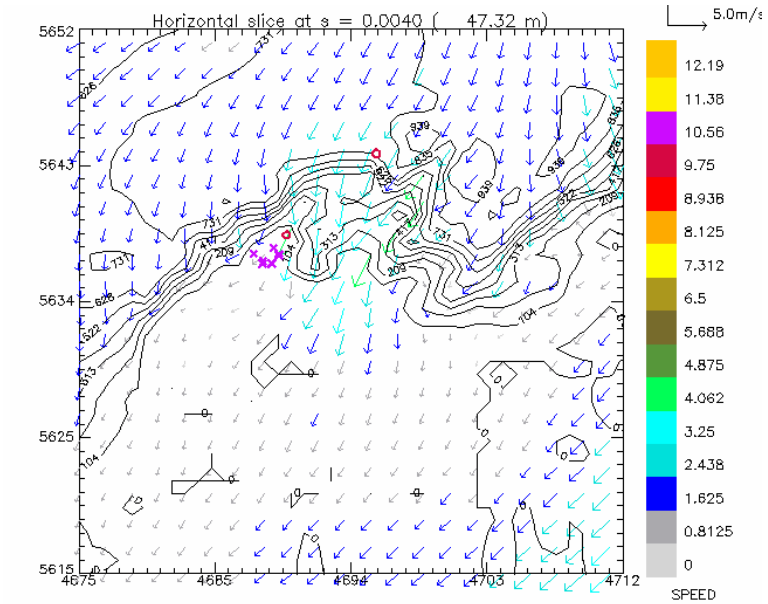

b

Figure 5. As in Figure 3 but for typical night-time situation with land breeze

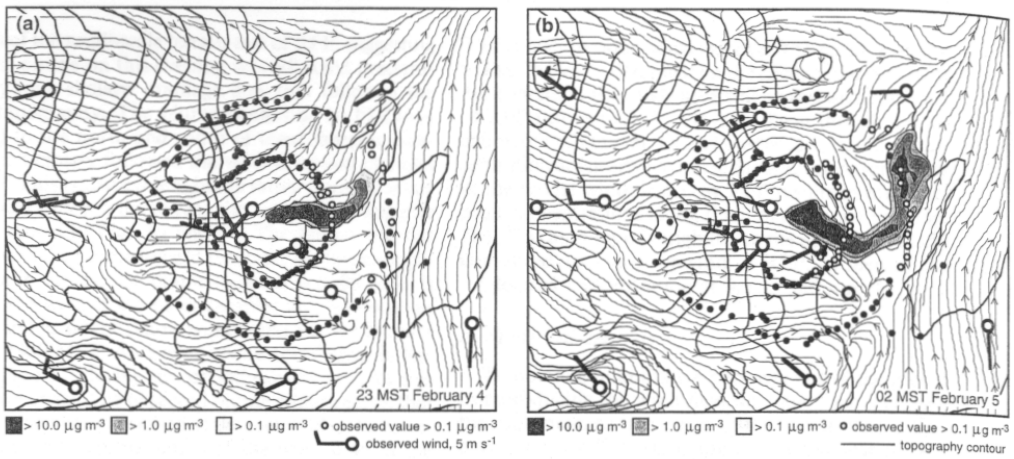

Figure 6. Wind field (streamlines) 26m AGL at (a) 2300 MST, 4 February 1991 with hourly-averaged surface concentration between 2300 and 0000 MST and (b) 0200 MST 5 February 1991 with hourly-averaged surface concentration between 0200 and 0300 MST. From Fast (1995).

3.6.3 Animation of LSM Simulation

An animation of a three-dimensional simulation in coastal complex terrain showing particle dispersion and contours of ground-level concentrations from two point sources can be viewed by double-clicking on Figure 7. The simulation using the model TAPM (Hurley, 1999; Hurley et al. 2001) begins at midnight and continues for 24 hours (the time in the top left-hand corner shows days, hours and minutes). Terrain is shaded according to elevation, and sea areas are coloured blue. Emissions released at a height of 100 m from the two coastal sources are transported offshore by the prevailing synoptic wind and return over land early afternoon in the sea breeze. Towards the end of the simulation, they are channelled to the northwest along a valley. Particles at all heights are displayed and this is why particles are moving in different directions at any one time. For example, low-level particles can be seen moving inland in the sea breeze, while others at higher levels are moving offshore in the synoptic wind, enhanced by the return flow of the sea-breeze circulation. Note that many more particles are used to calculate the concentrations than are used to visualise the dispersion.

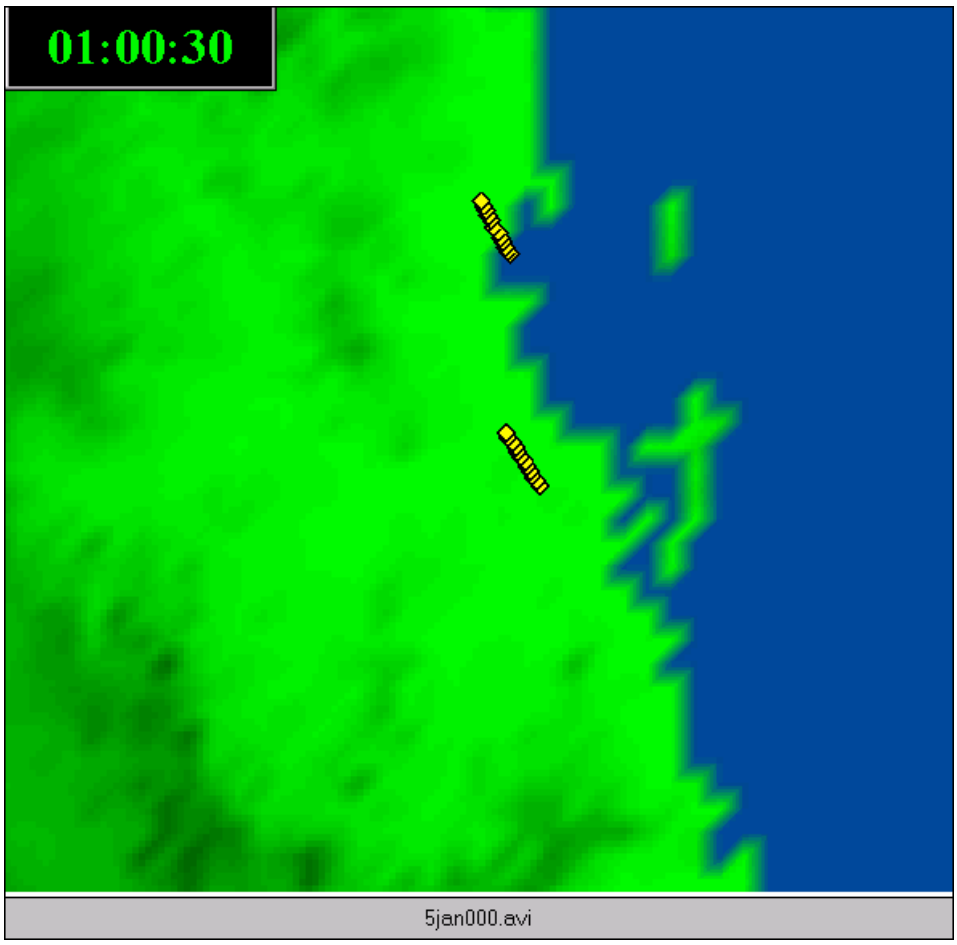

Figure 7. Animated dispersion of emissions from point sources using a prognostic three-dimensional air quality model TAPM.

3.7 Long-Range Transport (S. Trini Castelli)

International frontiers are disregarded by pollutants dispersing through the atmosphere. The Chernobyl accident at the end of April 1986 abruptly reminded the modellers' community of the importance of improving the reliability of models for long-range transport. The main limitation to this kind of study was the lack of experimental data, against which to perform the model validation, and of a common protocol for the evaluation of the results. An important step in developing this framework was the ATMES (Atmospheric Transport Model Evaluation Study) Project, where a quality-controlled database of the measurements collected for the case of the Chernobyl accident was assembled and made available. The results of this study were affected by the uncertainties in the source term and by the heterogeneity of the observed data, due to the accidental conditions of the release. To overcome these deficiencies, in 1992 the field experimental campaign ETEX (European Tracer EXperiment) was carried out. Tracer releases under controlled conditions and systematic monitoring enabled model validation and intercomparison studies, even for the case of emergency response. A common evaluation protocol was also set up. In this section, ATMES

and ETEX studies are described and the results obtained by the Lagrangian particle models are summarised and briefly discussed. For the identification, classification and description of the other participating models, refer to the relative official literature cited in the sub-sections.

3.7.1 The ATMES Project

The ATMES Project was initiated in November 1986 by a collaboration of IAEA (International Atomic Energy Agency) and WMO (World Meteorological Office), while CEC (Commission of European Community) joined the initiative in 1987 through the JRC (Joint Research Centre). The purpose of ATMES was to review and to intercompare pollutant dispersion models for the atmosphere in order to identify the most promising approaches for the modelling of the long-range transport of radionuclides and to provide a guidance for future work. The area considered for the exercise, from 10°W to 40° E and 35°N to 70°N, included most of the European measuring stations for which radiological data were available.

The data set supplied for the exercise contained:

- the estimated source term for the Chernobyl plant (51° 17' N, 30° 15' E) consisting of release data in TBq/day for I^{131} and Cs^{137}, together with an estimate of the effective height of the initial plume centre-of-mass,
- ECMWF meteorological data (wind components, temperature and relative humidity on pressure levels, wind at 10 m height, surface pressure, temperature at 2 m height, total cloud cover) consisting of analyses (for the period between 25th April 12:00 to 10th May 18:00 UTC, with 6 hours time interval and 1.125 degrees resolution, on the area from 81°W to 40.5° E and from 29.25 ° to North pole) and of forecasts (between 25th April 12:00 to 30th April 12:00);
- KNMI precipitation data from 25th April to 14th May;
- list of the locations of the measuring stations, referring to I^{131} and Cs^{137} air concentration and Cs^{137} daily deposition

The model results, in terms of air concentrations of I^{131} and Cs^{137}, Cs^{137} wet and cumulative deposition were requested for a period of 14 days. A large number of modellers, 21, participated in the exercise, so that a statistical methodology was adopted to perform the model intercomparison (Klug et al., 1992). The ranking was performed separately for each data set according to several statistical parameters, like bias, Pearson correlation coefficient, NMSE (Normalised Mean Square Error), Standard Deviation, FA2 and FA5 (Fraction of calculated values within a factor of 2 and 5), FOEX (Factor of Exceedance, that is an absolute overestimation), FMT (Figure of Merit in Time), FMS (Figure of Merit in Space) and Kolmogorov-Smirnov test. The criteria adopted for the ranking was to give equal importance to the different statistical parameters, so that an equal weight was associated with each of them in summing up to obtain a total score.

The seven Lagrangian particle models that participated in the intercomparison are listed in Table 1. To single out the quality of their performances among the other

models, Table 2 lists the five models providing the best results for the different data sets.

Table 1. List of the Lagrangian particle models in ATMES.

ATMES Model Number	Model Name	Organisation
4	ADPIC	LLNL (Lawrence Livermore Laboratory, USA)
5	APOLLO	ENEA-DISP (Committee for Research and Development of Nuclear and Alternative energies, I)
8	SPEEDI	JAERI (Japan Atomic Energy Research Institute, J)
9		JMRI (Japan Meteorological Research Institute, J)
11	JMA-GTTM	JMA (Japan Meteorological Agency, J)
18		IAG (Institute of Applied Geophysics, USSR)
20	NAME	MO (Meteorological Office, UK)

Table 2. ATMES statistical ranking for the data subsets: first five models E=Eulerian, L=Lagrangian puff, LP=Lagrangian Particle.

Sample Size	I^{131} air concentration *700*	Cs^{137} air concentration *700*	Cs^{137} daily deposition *140*	Cs^{137} cumulated deposition *95*	I^{131} forecasted wind field *35*	Cs^{137} forecasted wind field *35*
RANK	Model Number and Type					
I	5 (LP)	7 (E)	3 (L)	4 (LP)	2 (E)	10 (E)
II	18 (LP)	5 (LP)	18 (LP)	21 (L)	17 (L)	7 (E)
III	7 (E)	15 (L)	15 (L)	8 (LP) 15 (L)	5 (LP)	2 (E)
IV	17* (L)	19 (L)	4 (LP)	10 (E)	10 (E)	5 (LP)
V	21 (E)	10 (E)	5 (LP)	17 (L)	8 (LP)	15 (L) 17 (L)

*model n. 17 is a Lagrangian segmented-plume model

In Table 3 the ranks corresponding to the total score of the five best models are reported, for both the analysed and forecast meteorological input fields. This ranking has been obtained summing up the partial scores of the models from the different data subsets. Three models did not supply a full information about the depositions. The results obtained using the forecasts were provided by ten models.

Table 3. ATMES statistical ranking for the total data: first five models E=Eulerian, L=Lagrangian puff, LP=Lagrangian Particle.

RANK	Analysis Meteo Input	Forecast Meteo Input
	Model Number and Type	
I	5 (LP)	2 (E)
II	4 (LP) 15 (L)	10 (E)
III	17 (L)	7 (E)
IV	18 (LP)	5 (LP)
V	7 (E)	17 (L)

No systematic trend in model performances was evident, with Eulerian and Lagrangian models attaining the same average ranking, and nor was there evidence of a correlation between the complexity of the models and improved results. The outcomes of the analysis of the results showed that the cloud trajectories were generally well predicted when using the analysed wind field, while the deterioration of performances when using the forecasted fields was related to the strong dependency of the result quality on the meteorological input data. Improvement in space and time resolution and in the quality of the meteorological and precipitation data was recommended. From Table 3 it can be seen that a good quality contribution was given by the Lagrangian particle models using the analysed fields. As regards the model sensitivity to simulation parameters, the necessity of improving the description of the boundary layer structure, including the interaction of the pollutant cloud with it, and of the deposition parameters was recognised.

Considering the uncertainty and lack of information of the Chernobyl case, the final recommendation of the conclusive ATMES workshop in 1991 was that '(…) *a controlled release experiment in Europe be launched by releasing from a given location a tracer which can be detected at very large distances*' (Klug et al., 1992).

3.7.2 The ETEX Project

The ETEX Project too was sponsored by EC, WMO and IAEA and was aimed at evaluating the ability of meteorological services and research institutions to predict in real time the atmospheric dispersion of inert pollutants over large distances (Nodop, 1997). Two tracer releases were carried out on 23 October and 14 November 1994, for a release period of nearly 12 hours, an ETEX modelling phase was performed in parallel with the experiment. The source was set in Monterfil (2° W, 48°3' N, 90m asl, France) and the sampling domain almost covered from 43° to 60° N and 2° to 25° E. When the release started, the 28 modellers, previously alerted, were notified of the starting time, source location and emission rate. The models were run in real-time to predict the evolution of the tracer cloud and the predictions were sent to the statistical evaluation team as available. In Table 4 the Lagrangian particle models participating in the real-time phase in ETEX are listed.

Table 4. List of the Lagrangian particle models in ETEX real-time phase.

ETEX real-time Model Name	Organisation
LPDM	DWD (German Weather Service, D)
APOLLO	ANPA (National Agency for Environment, I)
ADPIC	LLNL (Lawrence Livermore Laboratory, USA)
WSPEEDI	JAERI (Japan Atomic Energy Research Institute, J)
NAME II	MetOff (Meteorological Office, UK)
SNAP	NMI (Norwegian Meteorological Institute, N)
LPDM	SRS (Westinghouse Savannah River Laboratory, USA)
STADIUM	TYPHOON (RU)
	KMI (Royal Institute of Meteorology , B)
TRADOS	FMI (Finnish Meteorological Institute, Fi)

For ETEX, statistical measures used in the ATMES case were augmented by the Geometrical Mean Bias (MG) and the Geometric Mean Variance (VG). The statistical analysis of results from the first release showed that a group of models were able to forecast in real time the cloud position and its horizontal extent up to a period of 48 hours, although the forecast worsened for later times. The concentration evolution at the stations was not always correctly reproduced, not even by the best models. A group of 6 models showed excellent performances, 8 models had few excellent and some average performances and 4 models had intermediate results. In the second experiment the presence of the ground level tracer cloud was limited to 24 hours after the release and the number of non-zero measurements restricted the statistics to few parameters. None of the participant models was able to simulate correctly the ground level concentrations, neither spatially nor as time evolution. The general model trend was to greatly over-predict the concentrations.

From the analysis of ETEX real-time results, it was not possible to attribute the differences between measurements and predictions specifically to the meteorological or the dispersion phases. Also in order to relate the differences in observed and calculated concentrations to the dispersion simulation, the **ATMES II modelling exercise** was launched almost two years after the ETEX campaign (Mosca et al., 1998; Girardi et al., 1998). The exercise was open to all the long-range modellers and participants were required to calculate the concentration field of the ETEX first tracer experiment using a common meteorological input data set, corresponding to the ECMWF analysis for the ETEX period, but also models using non-ECMWF data were considered. The total number of models participating in ATMES II was 49, 35 of them using ECMWF analyses (coded from 101 to 135) and 14 using non-ECMWF data (coded from 201 to 214). In 5 the Lagrangian particle models participating in ATMES II are listed.

Table 5. List of the Lagrangian particle models in ATMES II.

ATMES II Model Number	Model Name	Organisation
101	FLEXPART	IMP (Univ. Wien, Institute of Meteorology and Physics, A)
106	LPDM	DWD (German Weather Service, D)
107	LPDM	DWD (German Weather Service, D)
112	DIFPAR	EDF (French Electricity, F)
113	APOLLO	ANPA (National Agency for Environment, I)
114	MILORD	ICGF/CNR (National Research Council, I)
115	WSPEEDI	JAERI (Japan Atomic Energy Research Institute, J)
116	MRI-LTM	MRI (Meteorological research Institute, J)
118	MATHEW/ ADPIC	FOA (Defence Research Establishment, S)
119	NAME	MetOff (Meteorological Office, UK)
131	SNAP	DNMI (Norwegian Meteorological Institute, N)
132	LPDM	SRS (Westinghouse Savannah River Laboratory, USA)
203	LPDM	DWD (German Weather Service, D)
207	MRI-LTM	MRI (Meteorological research Institute, J)
209	NAME	MetOff (Meteorological Office, UK)
210	NAME	MetOff (Meteorological Office, UK)
213	SNAP	DNMI (Norwegian Meteorological Institute, N)

The statistical analysis of the results was performed on the same parameters as for the ETEX real-time phase and divided into three stages: a *time analysis*, considering concentrations at a fixed location for the whole duration of the episode, a *space analysis*, considering concentrations at a fixed time all over the domain, and a *global analysis*, where all the concentration values at any time and location are considered. In Table 6 the ranking of models based on the global

analysis is reported, giving to each statistical index the same weight as in the statistics performed for ATMES and ETEX projects. The rank is given for the different groups separately and then for the total of the models. In the second column are listed the first ten models in the statistical ranking for the group ECMWF (35 models), in the third column there are the first five models for the non-ECMWF data models (14) and in the fourth column the first ten models over the total of models (49) are ranked.

As an overall result, a general substantial improvement in ATMES II over those from ETEX real-time phase was found. This was expected on account of the better resolution of the meteorological fields used and the elapsed time between the two exercises, during which improvement in models and tunings of key parameters were possible.

Considering that the participating Lagrangian particle models were 17 out of 49 and that in the ranking of the total models eight of them are in the first ten, a good performance of this kind of models can be recognised in long-range dispersion modelling.

Table 6. ATMES II exercise: statistical ranking E=Eulerian, L=Lagrangian, LP=Lagrangian Particle, sL=semi-Lagrangian.

RANK	ECMWF Meteo Input Models	Non-ECMWF Meteo Input Models	All Models
Model Number and Type			
I	107 (LP)	209 (LP)	107 (LP)
II	111 (sL)	210 (LP)	111 (sL)
III	131 (LP)	208 (E)	209 (LP)
IV	115 (LP)	203 (LP)	203 (LP)
V	114 (LP)	213 (LP)	114 (LP)
VI	127 (E-L)		210 (LP)
VII	101 (LP)		131 (LP)
VIII	112 (LP)		208 (E)
IX	128 (E)		115 (LP)
X	134 (L)		101 (LP)

3.8 Footprint Analysis of Scalar Fluxes (A. Luhar)

Any surface source, located at (*x'*, *y'*, 0), can potentially contribute to the vertical flux F (with units of g m^{-2} s^{-1} for example) of a scalar measured downwind at point (x, y, z_m). The term footprint, f, is defined as the contribution, per unit surface flux, of each unit element of the upwind surface area to the measured vertical flux (Horst and Weil, 1992)

$$F(x,y,z_m) = \int_{-\infty}^{\infty}\int_{-\infty}^{x} Q_o(x',y',0)\; f(x-x',y-y',z_m)\, dx'dy' \qquad (80)$$

where Q_o is the surface emission flux (g m^{-2} s^{-1}) of an area-source element located at (*x'*,*y'*) upwind of the measurement location. Equation (80) implies that the measured scalar flux is the integral of the contributions from all elements of upwind surface emissions, whereas the footprint (m^{-2}) is the relative weight given to each elemental source. In general, for a given location, f is a function of only the turbulent flow field that governs transport and diffusion.

Footprint estimation is useful for the identification of the sources of greenhouse gases, such as water vapour and methane that contribute to measured fluxes, and for assessing the relative importance of these sources. For many cases involving surface inhomogeneities, such as changes in surface roughness or moisture (e.g. transition from a relatively smooth arid area to an irrigated crop), footprint analysis can provide an estimate of the key 'height-to-fetch' ratio that determines the optimum sitting of instruments for flux measurements. It can also facilitate the interpretation of airborne flux measurements in relation to tower data.

Footprint analysis can often be performed in two dimensions when the source area is of large extent in the crosswind direction with respect to the flux measurement position. For such cases, Equation (80) can be written as

$$F(x,z_m) = \int_{-\infty}^{x} Q_o(x',0)\; f_2(x-x',z_m)\, dx' \qquad (81)$$

where f_2 (m^{-1}) is the two-dimensional footprint. In a region with nearly uniform surface conditions, Q_o can be assumed to be independent of *x'*.

Equation (81) suggests that the footprint f_2 is the vertical flux F_L (g m^{-2} s^{-1}) at the measurement point (x, z_m) due to a continuous line source of unit strength located upwind at (x', 0). Thus

$$f_2(x-x',z_m) = \frac{1}{Q_o}\frac{dF(x,z_m)}{dx'} = \frac{F_L(x,z_m)}{q} \qquad (82)$$

where q is the line source strength (g m^{-1} s^{-1}). Figure 8 presents a schematic diagram of the footprint of upwind sources that contribute to the flux measured at (x,z_m).

Analytical methods have been used to predict flux footprints using analytical solutions to the diffusion equation for horizontally homogeneous surface layers (e.g., Schuepp et al., 1990; Horst and Weil, 1992; Haenel and Grünhage, 1999). However, these methods are not valid when the surface-layer similarity is no longer applicable; for example, above the surface layer (relevant to aircraft data), within plant canopies, or when measuring fluxes from surfaces of limited extent (fetch), such as small lakes or irrigated fields within arid lands, so that the effects of the flow inhomogeneity are important. Under such conditions, Lagrangian stochastic dispersion models prove valuable in predicting the footprint. They are also useful for testing and improving footprint predictions obtained from the analytical solutions. Stochastic models have been used in the past for footprint predictions in the surface layer (Leclerc and Thurtell, 1990; Horst and Weil, 1992), in the convective boundary layer (Wilson and Swaters, 1991), for a step change in the surface roughness and moisture (Luhar and Rao, 1993), and within and over forest canopies (Baldocchi, 1997). Experimental evaluation of analytical and Lagrangian footprint models has been reported by Finn et al. (1996).

When the turbulent flow is horizontally homogeneous, the footprint f_2 at a given height depends only on the separation between the flux measurement point and the elemental source. However, when the flow is horizontally inhomogeneous, it depends on their actual locations. In the former case, footprints due to a single line source, calculated at several locations downwind of the source, can be used to derive the footprint at a particular location due to a number of line sources located upwind. For this purpose, particles are released at the surface from a crosswind line source of unit emission flux. Particle numbers and corresponding vertical velocities are computed at a number of heights and downwind distances, and are then used to determine the average vertical flux at these locations. This vertical flux is equal to the footprint f_2 [Equation (82)]. However, in the horizontally inhomogeneous flow case, one may not use this procedure; the footprints are calculated by placing a number of line sources upwind of the measurement point (e.g. Luhar and Rao, 1993). The Lagrangian stochastic models mentioned above are generally run in forward mode to determine the footprint. That is, particles are released at the source position, and the position and velocity distribution of particles reaching the receptor position is calculated. Flesch et al. (1995) and Flesch (1996) use a backward Lagrangian stochastic technique for footprint calculations, which is potentially more efficient and flexible than the forward Lagrangian stochastic technique. In the backward technique, particles are released at the receptor position and tracked backwards to determine their distribution at the ground to identify the sources contributing to fluxes at the receptor. However, this technique is not valid when the flow is horizontally inhomogeneous.

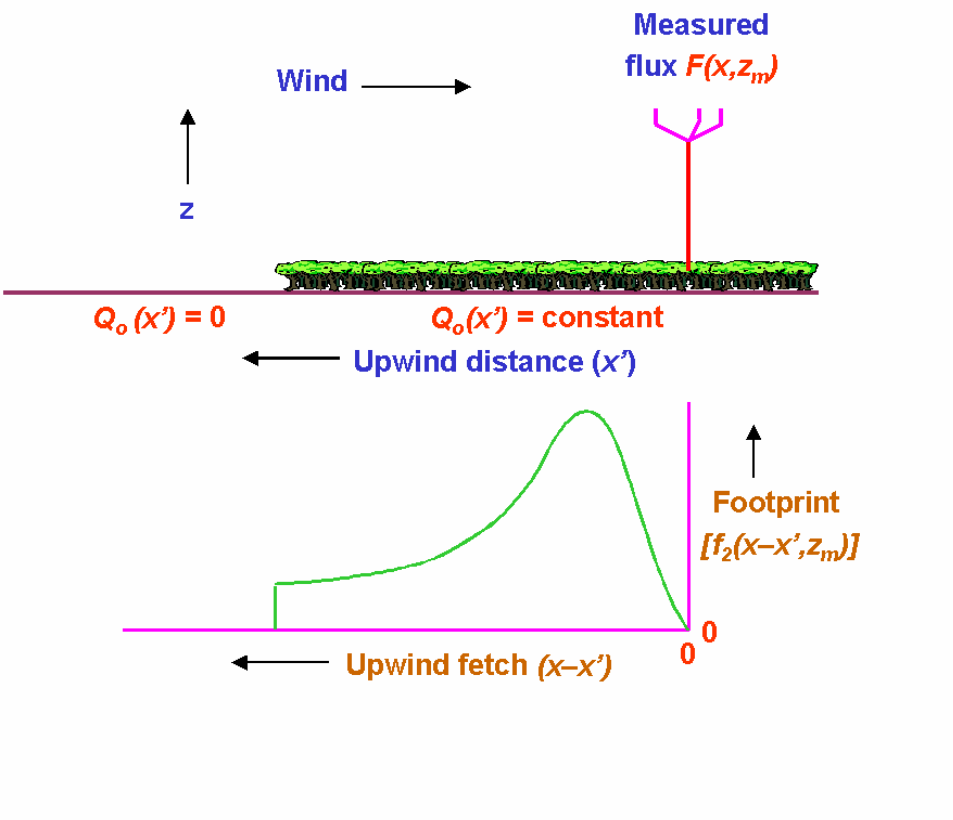

Figure 8. Schematic diagram showing the footprint of upwind sources for the flux measurements made at point (x,z_m) over a surface with simple inhomogeneity.

References

Anfossi D., Ferrero E., Sacchetti D. and S. Trini Castelli (1996). Comparison among empirical probability density functions of the vertical velocity in the surface layer based on higher order correlations. *Boundary Layer Meteorology*, **82**, 193-218

Anfossi, D., Ferrero, E., Tinarelli, G., and Alessandrini, S., (1997) A simplified version of the correct boundary conditions for skewed turbulence in Lagrangian particle models. *Atmospheric Environment*, **31**:301-308.

Anfossi, D., Desiato, F., Tinarelli, G., Brusasca,G., Ferrero, E. and Sacchetti D. (1998). TRANSALP 1989 experimental campaign –II. Simulation of a tracer experiment with Lagrangian particle models. *Atmospheric Environment*, **32**, 1157-1166.

Anfossi D., G. Degrazia, E. Ferrero, S.E. Gryning, M.G. Morselli and S. Trini Castelli, (2000). Estimation of the Lagrangian structure function constant C_0 from surface layer wind data, *Boundary Layer Meteorology*, **95**: 249-270

Anfossi (2000) Short Review of Lagrangian Stochastic Models for the Simulation of the Atmospheric Pollutant Dispersion. Hybrid Methods in Engineering, **2**, 261-279

Antonia R.A. and Atkinson J.D., (1973). High-order moments of Reynolds shear stress fluctuations in a turbulent boundary layer, *J. Fluid Mech.*, **58**, part 3, 581-593

Baerentsen J.H. and Berkowicz R. (1984). Monte-Carlo simulation of plume diffusion in the convective boundary layer, *Atmospheric Environment*, **18**, 701-712

Baldocchi, D., (1997). Flux footprints within and above forest canopies. *Boundary-Layer Meteorology* **85**, 273–292

Batchvarova E. and Gryning S.E. (1991). Applied model for the growth of the daytime mixed layer. *Boundary Layer Meteorology*, **56**, 261-274

Batchelor, G.K. (1949). Diffusion in a field of homogeneous turbulence, I: Eulerian analysis. *Aust. J. Sci. Res*., **2**, 437-450.

Borgas, M. S. and Sawford, B. L., (1994). A family of stochastic models for two-particle dispersion in isotropic homogeneous stationary turbulence. *Journal of Fluid Mechanics* **279**, 69–99.

Brusasca G., G. Tinarelli and D. Anfossi (1989). Comparison between the results of a Monte Carlo atmospheric diffusion model and tracer experiments. *Atmospheric Environment*, **23**, 1263 – 1280

Brusasca, G., G. Tinarelli, and D. Anfossi, (1992). Particle model simulation of diffusion in low wind speed stable conditions. *Atmospheric Environment*, **4**, 707-723

Buckley, R.L. and Kurzeja, R.J. (1997). An observational and numerical study of the nocturnal sea breeze. Part II: chemical transport. *J. Appl. Meteorol.*, **36**, 1599-1619.

Caughey, S.J. (1982). Observed characteristics of the atmospheric boundary layer, Atmospheric turbulence and air pollution modelling, F.T.M. Nieuwstadt and H. van Dop eds., Reidel, Dordrecht, 107-158.

Chock P. and S. Winkler (1994a). A particle grid air quality modelling approach. 1. The dispersion aspect, *Journal of Geophysical Research*, **99**, 1019-1031.

Chock P. and S. Winkler (1994b). A particle grid air quality modelling approach. 2. Coupling with chemistry, *Journal of Geophysical Research*, **99**, 1033-1041.

Cogan J.L. (1985). Monte Carlo simulation of a buoyant dispersion. *Atmospheric Environment*, **19**, 867-878

Crone G.C., Dinar N., van Dop H. and Verver G.H.L. (1999). A Lagrangian approach for modelling turbulent transport and chemistry, *Atmospheric Environment,* **33** (29), pp. 4919-4934.

Csanady G.T. (1973). *Turbulent diffusion in the environment*. Reidel

Davis P.A. (1983). Markov chain simulations of vertical dispersion from elevated sources into the neutral planetary boundary layer". Boundary-Layer Meteorology, **25**, 355-376

Deardorff, J.W. (1974). Three-dimensional numerical study of the height and mean structure of a heated planetary boundary layer. *Boundary Layer Meteorology*, **7**, 81-106.

Deardorff J. and G. Willis (1982). Ground-level concentrations due to fumigation into an entraining mixed layer, *Atmospheric Environment*, **16**, 1159-1170.

De Baas H.F., H. Van Dop, and F.T.M. Nieuwstadt, (1986). An application of the Langevin equation for inhomogeneous conditions to dispersion in a convective boundary layer. *Quart. J. Roy. Meteor. Soc*., **112**, 165-180

Degrazia G.A. and Anfossi D. (1998). Estimation of the Kolmogorov constant C_0 from classical statistical diffusion theory, *Atmospheric Environment*, **32**, 3611-3614

Degrazia, G., Anfossi, D., Carvalho, J.C., Mangia, C., Tirabassi, T., Campos Velho and H.F. (2000). Turbulence parameterisation for PBL dispersion models in all stability conditions. *Atmospheric Environment,* **34**, 3575-3583.

de Haan, P. (1999). On the use of density kernels for concentration estimations within particle and puff dispersion models. *Atmospheric Environment,* **33**, 2007-2021.

de Haan, P., and Rotach, M. W., (1998). A novel approach to atmospheric dispersion modelling: the puff-particle model. *Quarterly Journal of the Royal Meteorological Society,* **124**, 2771–2792.

Du (1997). Universality of the Lagrangian velocity structure function constant (C_0) across different kinds of turbulence. *Boundary Layer Meteorol*ogy, **83**, 207-219.

Du S., Wilson J.D. and Yee E. (1994). Probability density functions for velocity in the convective boundary layer and implied trajectory models, *Atmospheric Environment*, **28**, 1211-1217

Duran J., L. Romer, T. Duranova and M. Stubna, (1998). A Lagrangian statistical (Monte-Carlo) atmospheric dispersion model validation on the results of wind tunnel experiments *5th Conference on Harmonization within ADM for regulatory purposes 18-21 May, Rodos, Greece*

Durbin P.A. 1980, A stochastic model of two-particle dispersion and concentration fluctuations in homogeneous turbulence, J. Fluid Mech., **100**, 2, 279-302

Durbin P.A. and Petterson Reif A. (2001). Statistical theory and modeling for turbulent flows. John Wiley and Sons, 285 pp

Durst F., Jovanovic J. and Johansson T.G., (1992). On the statistical properties of truncated Gram-Charlier series expansions in turbulent wall-bounded flows. *Phys. Fluids*, **A 4**, 118-126

Eastman, J.L., Pielke, R.A. and Lyons, W.A. (1995). Comparison of lake-breeze model simulations with tracer data. *J. Appl. Meteorol.*, **34**, 1398-1418.

Eberhard, W.L., Moninger, W.R. and G.A. Briggs (1988). Plume dispersion in the convective boundary layer. Part I: CONDORS field experiment and example measurements. *J. Appl. Meteorol.*, **27**, 599-616.

Fast, J.D. (1995). Mesoscale modeling and four-dimensional data assimilation in areas of highly complex terrain. *J. Appl. Meteorol.*, **34**, 2762-2782.

Ferrero E., D. Anfossi, G. Brusasca and G. Tinarelli (1995). Lagrangian particle model (LAMBDA): evaluation against tracer data, *Int. J. Environment and Pollution*, **5**, 360-374.

Ferrero E. and Anfossi D. (1998a). Sensitivity analysis of Lagrangian Stochastic models for CBL with different PDF's and turbulence parameterizations. Air Pollution Modelling and its Applications XII, S.E. Gryning and N. Chaumerliac eds., Plenum Press, New York, **22**, 673-680.

Ferrero E. and Anfossi D. (1998b). Comparison of PDFs, closures schemes and turbulence parameterizations in Lagrangian Stochastic Models. Int. J. Environment and Pollution, **9**, 384-410.

Ferrero E., Anfossi D., Tinarelli G. and Trini Castelli S. (2000b). Lagrangian particle simulation of an EPA wind tunnel tracer experiment in a schematic two-dimensional valley. *Air Pollution Modelling and its Applications XIV*, S.E. Gryning and F.A. Schiermeier Eds., Plenum Press, New York.

*Ferrero E., D. Anfossi, G.Tinarelli and M. Tamiazzo, (2000a). Intercomparison of Lagrangian stochastic models based on two different PDFs Int. J. Environment and Pollution, **14**, 225-234*

Ferrero E., Anfossi D. and Tinarelli G. (2001). Simulations of Atmospheric Dispersion in Urban Stable Boundary Layer, Int. J. Environment and Pollution, **16**, 1-6

Finn, D., Lamb, B., Leclerc, M. Y. and Horst, T. W. (1996). Experimental evaluation of analytical and Lagrangian surface-layer flux footprint models. *Boundary Layer Meteorology*, **80**, 283-308.

Flesch T.K., Wilson D.J. and Yee E. (1995). Backward-Time Lagrangian Stochastic Dispersion Models and their Application to estimate Gaseous Emissions, *J Appl. Meteorol.*, **34**, 1320-1332.

Flesch, T. K., (1996). The footprint for flux measurements, from backward Lagrangian stochastic models. *Boundary Layer Meteorology*, **78**, 399–404.

Franzese P., A. Luhar and M. Borgas (1999). An efficient Lagrangian stochastic model of vertical dispersion in the convective boundary layer, *Atmospheric Environment*, **33**, 2337-2345.

Frenkiel F.N. and Klebanoff P.S., (1967). Higher order correlations in a turbulent field. *Phys. Fluids*, **10**, 507-520

Gaffen D.J., Benocci C. and Olivari D. (1987) Numerical modeling of buoyancy dominated dispersal using a Lagrangian approach. *Atmospheric Environment*, **21**, 1285-1293

Gardiner C.W. (1990). *Handbook of stochastic methods*. Springer Verlag.

Gifford, F. A., (1959). Statistical properties of a fluctuating plume dispersion model. *Advances in Geophysics*, **6**, 117–137.

Gifford F.A. (1960). Peak to average concentration ratios according to a fluctuating plume dispersion model. *Int. J. Air Pollut.*, **3**, 253-260.

Gifford F.A. (1982). Horizontal diffusion in the atmosphere: a Lagrangian-dynamical theory, *Atmospheric Environment*, **16**, 505-512.

Gingold, R.A., and J.J. Monaghan (1982). Kernel estimates as a basis for general particle methods in hydrodynamics. *J. Computational Phys.*, **46**:429-453.

Girardi F., Graziani G., van Velzen D., Galmarini S., Mosca S., Bianconi R., Bellasio R., Klug W. and Fraser G. (1998). The European Tracer Experiment. EUR 18143 EN.

Gronskei K.E. (1990). Variation in dispersion conditions with height over urban areas – Results of dual tracer experiments. *Proceedings from the Symposium on Turbulence and atmospheric Diffusion*, April 30 – May 2, Roskilde, Denmark, American Meteorological society, Boston, MA (USA).

Gryning S.E. and Batchvarova E. (1990). Simple model of the daytime boundary layer height. *Ninth Syposium on turbulence and Diffusion*. American Meteorological Society, 379.

Gryning S.E. (1999). Some aspects of atmospheric dispersion in the stratified atmospheric boundary layer over homogeneous terrain. *Boundary-Layer Met*., **90**, 479-494.

Haenel, H.-D. and L. Grünhage, (1999). Footprint analysis: a closed analytical solution based on height-dependent profiles of wind speed and eddy viscosity. *Boundary Layer Meteorology*, **93**, 395–409.

Hanna, S.R. (1968). A method of estimating vertical eddy transport in the planetary boundary layer using characteristics of the vertical velocity spectrum. *J. Atmos. Sci.*, **25**, 1026.

Hanna S.R. (1979). Some statistics of Lagrangian and Eulerian wind fluctuations. *J. Appl. Met*., **18**, 518-525.

Hanna, S.R. (1981). Lagrangian and Eulerian time-scale in the daytime boundary layer. *J. Appl. Meteorol.*, **20**, 242-249.

Hanna, S.R. (1982). Applications in air pollution modelling, Atmospheric Turbulence and Air Pollution Modelling, F.T.M. Nieuwstadt and H. Van Dop eds., Reidel, Dordrecht.

Hanna S. and R. Paine (1989). Hybrid plume dispersion model development and evaluation, *Atmospheric Environment*, **27A**, 1491-1508.

Hanna R.S., Bitter E.R. and Franzese P., (2001) The effect of roughness obstacles on flow and dispersion at industrial and urban sites, *Report AIChE CCPS Project 132*

Hernandez, J.F., Cremades, L. and Baldasano, J.M. (1995). Dispersion modelling of a tall stack plume in the Spanish Mediterranean coast by a particle model. *Atmospheric Environment*, **29**, 1331-1341.

Hibberd M. and B. Sawford (1994). A saline laboratory model of the planetary convective boundary layer, *Boundary Layer Meteorology*, **67**, 229-250.

Hibberd M. and A. Luhar (1996). A laboratory study and improved PDF model of fumigation into a growing convective boundary layer, *Atmospheric Environment*, **30**, 3633-3649.

Hinze J.O. (1975). *Turbulence*. Mc Graw Hill, 790 pp.

Holtslag, A.A. and Moeng, C.H. (1991). Eddy diffusivity and countergradient transport in the convective boundary layer. *J. Atmos. Sci.*, **48**, 1690-1698.

Horst, T. W. and J.C. Weil(1992). Footprint estimation for scalar flux measurements in the atmospheric surface layer. *Boundary Layer Meteorology,* **59**, 279–296.

Hurley P. (1994). PARTPUFF – A Lagrangian particle/puff approach for plume dispersion modelling applications, *J. App. Meteorology*, **33**, 285-294.

Hurley P.J. and Physick W.L. (1991). A Lagrangian particle model of fumigation by breakdown of the nocturnal inversion. *Atmospheric Environment*, **25A**, 1313-1325.

Hurley P. and W. Physick (1993a). A skewed, homogeneous Lagrangian particle model for convective conditions, *Atmospheric Environment*, **27A**, 619-624.

Hurley P. and W. Physick (1993b). Lagrangian particle modelling of buoyant point sources – plume rise and entrapment in convective conditions, *Atmospheric Environment*, **27A**, 1579-1584.

Hurley, P. (1997). An evaluation of several turbulence schemes for the prediction of mean and turbulent fields in complex terrain. *Boundary Layer Meteorology,* **83**, 43-73.

Hurley, P. (1999). The Air Pollution Model (TAPM) Version 1: Technical Description and Examples. CSIRO Atmospheric Research Technical Paper No. 43.

Hurley P., Blockley A., and Rayner K. (2001). Verification of a prognostic meteorological and air pollution model for year-long predictions in the Kwinana region of Western Australia. *Atmospheric Environment,* **35** (10): 1871-1880.

Irwin, J.S. (1979a). Estimating plume dispersion – a recommended generalized scheme. Preprints Fourth Symposium on Turbulence, Diffusion and Air Pollution. Am. Meteorl. Soc., 45 Beacon street, Boston Mass. 02108, 62-69.

Kaimal, J.C., Wyngaard, J.C., Haugen, D.A., Cote', O.R., Izumi, Y., Caughey, S.J. and Readings, C.J. (1976). Turbulence structure in the convective boundary layer. *J. Atmos. Sci.*, **33**, 2152-2169.

Kaimal, J.C.R., Eversole, D., Lenschow, D.H., Stankov, B.B., Kahn, P.H. and Businger, J.A. (1982). Spectral characteristics of the convective boundary layer over uneven terrain. *J. Atmos. Sci*., **39**, 1098-1114.

Kaimal, J.C. and Finnigan, J.J. (1994). Atmospheric boundary layer flows, Oxford University Press, 289 pp.

Kalthoff, N., Binder H.J., Kossman M., Vögtlin R., Corsmeier U., Fiedler F. and Schlager H. (1998). Temporal evolution and spatial variation of the boundary layer over complex terrain, *Atmospheric Environment*, **32**, 1179-1194.

Kendall M. and Stuart A. (1977), *The advanced theory of statistics*, MacMillan, New York.

Kerschgens M.J, Nolle C. and Martens R. (2000) Comments on turbulence parameters for the calculation of dispersion in the atmospheric boundary layer. *Meteorologische Zeitschrft*, **9**, 155-163

Kerr A.F.S, Anfossi, D., Carvalho, Jonas C. and Trini Castelli, S. (2001a). A Dispersion Study of the Aerosol Emitted by Fertilizer Plants in the Region of Serra do Mar Sierra, Cubatão, Brazil, *Int. J. Environment and Pollution*, **16**, 251-263

Kerr A., Anfossi D., Trini Castelli S. and Nascimento S.A. (2001b). Investigation of inhalable aerosol dispersion at Cubatão by means of a modelling system for complex terrain". *Hybrid Methods in Enginnering*, **2**, 389-407

Khurshudyan L.H., Snyder W.H. and Nekrasov I.V., (1981). Flow and dispersion of Pollutants within Two-Dimensional Hills, EPA REPORT No. -6000/4-81/067.

Khurshudyan L.H., Snyder W.H., Nekrasov I.V., Lawson R.E., Thompson R.S and Schiermeier F.A., (1990). Flow and Dispersion of Pollutants within Two-Dimensional Valleys, *Summary Report on Joint Soviet-American Study, EPA REPORT* No. 600/3-90/025

Klug W., Graziani G., Grippa G., Pierce D. and Tassone C. Eds. (1992). Evaluation of Long Range atmospheric Transport Models using Environmental radioactivity Data from the Chernobyl Accident. The ATMES Report. EUR 14147 EN.

Klug W. (2000). What did we learn from the ETEX Experiment?. *Proceedings of the* Millennium NATO/CCMS International Technical Meeting on Air Pollution Modelling and its Application, Boulder (Colorado, USA) 15-19 May 2000, AMS Ed., 256-268.

Lamb, R.G., H. Hogo, and L.E. Reid (1979). A Lagrangian approach to modelling air pollution dispersion: Development and testing in the vicinity of a roadway. EPA Research Report EPA-600/4-79-023.

Leclerc, M. Y. and G.W. Thurtell (1990). Footprint prediction of scalar fluxes using a Markovian analysis. *Boundary Layer Meteorology,* **52,** 247–258.

Legg B.J. and Raupach M.R. (1982). Markov-chain simulations of particle diffusion in inhomogeneous flows: the mean drift velocity induced by a gradient in Eulerian velocity variance. *Boundary Layer Meteorology,* **24**, 3-13.

Ley A.J. (1982). A random walk simulation of two dimensional turbulent diffusion in the neutral surface layer. *Atmospheric Environment*, **16**, 2799-2808.

Lorimer, G.S. (1986). The kernel method for air quality modelling: I. Mathematical foundation. *Atmospheric Environment,* **20**:1447-1452.

Luhar A.K., and Britter R.E. (1989). A random walk model for dispersion in inhomogeneous turbulence in a convective boundary layer. *Atmospheric Environment*, **23**, 1191-1924.

Luhar, A.K. and Rao, K.S. (1993). Random-walk model studies of the transport and diffusion of pollutants in katabatic flows. *Boundary Layer Meteorology,* **66**, 395-412.

Luhar, A.K. and Rao, K.S. (1994). Lagrangian stochastic dispersion model simulations of tracer data in nocturnal flows over complex terrain. *Atmospheric Environment*, **21**, 3417-3431.

Luhar A. and B. Sawford (1995). Lagrangian stochastic modelling of the coastal fumigation phenomenon, *J. Appl. Meteorol.*, **34**, 2259-2277.

Luhar A., M. Hibberd, and P. Hurley (1996). Comparison of Closure Schemes used to Specify the Velocity PDF in Lagrangian Stochastic Dispersion Models for Convective Conditions, *Atmospheric Environment*, **30**, 1407-1418.

Luhar, A. K., Hibberd, M. F. and Borgas, M. S., (2000). A skewed meandering plume model for concentration statistics in the convective boundary layer. *Atmospheric Environment*, **34**, 3599-3616

Lyons, W.A., Pielke, R.A., Tremback, C.J., Walko, R.L., Moon, D.A. and Keen, C.S. (1995). Modeling impacts of mesoscale vertical motions upon coastal zone air pollution dispersion. *Atmospheric Environment*, **29**, 283-301.

Mahrt L. (1999). Stratified atmospheric boundary layers. *Boundary Layer Meteorology,* **90**, 375-396.

Maryon, R.H. and Buckland, A.T. (1994). Diffusion in a Lagrangian multiple particle model: a sensitivity study. *Atmospheric Environment*, **28**, No. 12, 2019-2038.

McNider R. (1981). Investigation of the impact of topographic circulations on the transport and dispersion of air pollutants, PhD Dissertation, Department of Environmental Sciences, University of Virginia, Charlottesville.

McNider, R.T. and Pielke, R.A. (1981). Diurnal boundary-layer development over sloping terrain. *J. Atmos. Sci.*, **38**, 2198-2212.

McNider, R.T., Moran, M.D. and R.A. Pielke (1988). Influence of diurnal and inertial boundary-layer oscillations on long-range dispersion. *Atmospheric Environment*, **22**, 2445-2462.

Monin A.S. and Yaglom A.M., (1965). *Statistical fluid mechanics: mechanics of turbulence*. Vol.1, MIT Press, p.225.

Mosca S., Bianconi R., Bellasio R., Graziani G. and Klug W. (1998). ATMES II – Evaluation of Long-range Dispersion Models using data of the 1st ETEX release. EUR 17756 EN.

Nasstrom, J.S. and D.L. Ermak (1999a). A homogeneous Langevin equation model, Part I: simulation of particle trajectories in turbulence with a skewed velocity distribution. *Boundary-Layer Meteorol*., **92**, 343-369.

Nasstrom, J.S. and D.L. Ermak (1999b). A homogeneous Langevin equation model, Part II: simulation of dispersion in the convective boundary layer. *Boundary-Layer Meteorol*., **92**, 371-405.

Nodop K, Ed (1997). ETEX Symposium on Long-Range Atmospheric Transport, Model Verification and Emergency Response. *Proceedings of the* ETEX Symposium, Wien (Austria), 13-16 May 1997, EUR 17346 EN.

Noonan, J.A., Physick, W.L., Carras, J. and D. Williams, (1994). Dispersion modelling and observations from elevated sources in coastal terrain, pp 533-540. *Air Pollution Modelling and its Application X*, Edited by S-V. Gryning and M.M. Millan, Plenum Press, New York.

Obukhov (1959). Description of turbulence in terms of Lagrangian variables. Adv. Geophys., 6, 113-116.

Oettl, D., R. A. Almbauer, and P. J. Sturm, (2001). A new method to estimate diffusion in stable, low wind conditions,. *J. of Appl. Meteor.*, 40, 259-268

Olesen H.R. (1995). Datasets and protocol for model validation *Int. J. Environment and Pollution,* **5**, N. 4-6, 693-701.

Olesen H. (1998). Tools for model validation. In: S.E. Gryning and N. Chaumerliac eds., *Air pollution modelling and its applications, XII*, Plenum Press, New York, 665-672.

Panofsky, H.A., Tennekes, H., Lenschow, D.H. and Wyngaard, J.C. (1977). The characteristics of turbulent velocity components in the surface layer under convective conditions. *Boundary Layer Meteorology,* **11**, 335-361.

Pearson, K. (1894). Contributions to the mathematical theory of evolution, Philosophical Transactions of the Royal Society of London, **185 - Part I**, 71-110.

Physick W.L., Noonan J.A., Manins P.C, Hurley P.J. and .H. Malfroy (1994a). Application of coupled prognostic windfield and Lagrangian dispersion codes for air quality purposes in a region of coastal terrain. Air Pollution Modelling and its Applications IX, H. Van Dop and G. Kallos eds., Plenum Press, New York.

Physick, W.L., J.A. Noonan, J.L. M^{c}Gregor, P.J.Hurley, D.J. Abbs and P.C. Manins (1994b). LADM: A Lagrangian Atmospheric Dispersion Model. *CSIRO Division of Atmospheric Research Technical Report No. 24*, 146pp.

Physick, W.L., Hurley, P.J. and P.C. Manins, (1995). Environmental impact assessment of industrial development at Gladstone, Australia. *Int. J. Environment and Pollution,* **5**, 548-556.

Physick, W.L. (1996). Photochemical smog studies in Australian cities, *Urban Air Pollution, Vol.2*, H. Power and N. Moussiopoulos, Eds., Computational Mechanics Publications, Southampton, Boston, pp. 141-184.

Pielke R.A., Cotton W.R., Walko R.L., Tremback C.J., Lyons W.A., Grasso L.D., Nicholls M.E., Moran M.D., Wesley D.A., Lee T.J. and Copeland J.H., (1992). A Comprehensive Meteorological Modeling System -RAMS. *Meteorology and Atmospheric Physics*, **49**, 69-91.

Poulos, G.S. and Bossert, J.E. (1995). An observational and prognostic numerical investigation of complex terrain dispersion. *J. Appl. Meteorol.*, **34**, 650-669.

Reid J.D (1979). Markov chain simulations of vertical dispersion in the neutral surface layer for surface and elevated releases. *Boundary Layer Meteorology,* **16**, 3-22

Reynolds, A.M. 1998, Comments on the Universality of the Lagrangian velocity structure function constant (Co) across different kinds of turbulence, *Boundary-Layer Meteorology, **89***, 161-170

Ries R., Heil O. and Wichmann-Fiebig M. (1997). Intercomparison of Lagrangian dispersion models and validation with Lillestrøm data *Int. J. Environment and Pollution*, **8**, 3-6.

Robinson, J., Mahre, Y. and E.Wakshal. (1992). The effects of mesoscale circulation on the dispersion of pollutants (SO_2) in the eastern Mediterranean, southern coastal plain of Israel. *Atmospheric Environment*, **26B**, 271-277.

Rodean, H.C. (1994). Notes on the Langevin model for turbulent diffusion of "marked" particles. Techn. Report UCRL-ID-115869, Lawrence Livermore National Laboratory, 122 pp.

Rodean H.C. (1996). Stochastic Lagrangian models of turbulent diffusion. Meteorological Monographs, 26, Amer. Met. Soc., Boston, USA.

Rotach M. (1998). Urban simulation of the Lillestrøm and Indianapolis data sets 5th Conference on Harmonization within ADM for regulatory purposes 18-21 May, Rodos, Greece.

Rotach M., S. Gryning and C. Tassone (1996). A two-dimensional Lagrangian stochastic dispersion model for daytime conditions, *Q. J. R. Meteorol. Soc.*, **122**, 367-389.

Rotach, M.W and de Haan, P.: 1997, 'On the Urban Aspect of the Copenhagen Data Set', *Int. J. Environment and Pollution*, **8**, Nos. 3-6, 279-286.

Rotach, M.W.: 1999, 'On the Influence of the Urban Roughness Sublayer on Turbulence and Dispersion', *Atmospheric Environment,* **33**, 4001–4008

Rotach, M.W.: 2001, 'Simulation of urban-scale dispersion using a Lagrangian stochastic dispersion model', *Boundary-Layer Meteorology,* **99**, 379-410

Sagendorf, J. F., and C. R. Dickson, (1974). Diffusion Under Low Windspeed, Inversion Conditions. *NOAA Technical Memorandum ERL ARL-52, National Oceanic and Atmospheric Administration*, Air resources laboratory 1750 Foote Drive, Idaho Falls, Idaho 83402, 89 pp.

Sawford B.L. (1985). Lagrangian simulation of concentration mean and fluctuation fields. *J. Clim. Appl. Met*., **16**, 3-22.

Sawford B. and F. Guest (1987). Lagrangian stochastic analysis of flux-gradient relationships in the convective boundary layer, *J. Atmos. Sci.*, **44**, 1152-1165.

Sawford B.L. and Guest F.M., (1988). Uniqueness and universality of Lagrangian stochastic models of turbulent dispersion, *8th Symposium on Turbulence and Diffusion*, San Diego, CA, A.M.S., 96-99.

Sawford B.L. (1991). Reynolds number effects in Lagrangian stochastic models of turbulent dispersion. *Phys. Fluids*, **A3**, 1577-1566.

Sawford B.L. (1993). Recent developments in the Lagrangian stochastic theory of turbulent dispersion. *Boundary Layer Meteorology,* **62**, 197-215.

Sawford B.L. and Borgas M.S. (1994). On the continuity of stochastic models for the Lagrangian velocity in turbulence. *Physica D,* **76**, 297-311.

Sawford, B., A. Luhar, J. Hacker, S. Young, I.-H. Yoon, J. Noonan, J. Carras, D. Williams and K. Rayner (1998). The Kwinana coastal fumigation study: I-Program overview, experimental design and selected results, *Boundary Layer Meteorology,* **89**, 359-384.

Schuepp, P. H., Leclerc, M. Y., MacPherson, J. I. and R.L. Desjardins (1990). Footprint prediction of scalar fluxes from analytical solutions of the diffusion equation. *Boundary Layer Meteorology,* **50**, 355–373.

Segal, M., Pielke, R.A., Arritt, R.W., Moran, M.D., Yu, C-H and Henderson, D. (1988). Application of a mesoscale atmospheric dispersion modeling system to the estimation of SO_2 concentrations from major elevated sources in southern Florida. *Atmospheric Environment*, **22**, 1319-1334.

Smith F.B. (1968). Conditional particle motion in a homogeneous turbulent field. *Atmospheric Environment*, **2**, 491-508.

Sorbjan, Z. (1989). Structure of the atmospheric boundary layer. Prentice Hall, New Jersey, 317 pp.

Stohl, A. and Thomson, D.J., 1999. A density correction for Lagrangian particle dispersion models. *Boundary-Layer Meteorology* **90**, 155-167.

Stull, R.B. (1988). An introduction to Boundary Layer Meteorology, Kluwer Academic Publishers, Boston, 666 pp.

Sun, W.Y. (1993). Numerical simulation of a planetary boundary layer. Part I: Cloud-free case. *Beitr. Phys. Atmos.*, **66**, 3-16.

Tassone C., Gryning S.E. and Rotach M., (1994). A random walk model for atmospheric dispersion in the daytime boundary layer. In: *Air Pollution Modeling and Its Application X*, S.E.Gryning and Millan M. Millan editors, Plenum Press, 243-251.

Taylor G.I. (1921). Diffusion by continuous movements. Proc. London Math. Soc., Ser. 2, **20**, 196-211.

Tennekes H. (1982). Similarity relations, scaling laws and spectral dynamics In: Atmospheric turbulence and air pollution modelling (edited by F.T.M. Nieuwstadt and H. van Dop), Reidel, Dordrecht, 37-68.

Thomson D.J. (1984). Random walk modelling of diffusion in inhomogeneous turbulence. *Quart. J. Roy. Meteor*. Soc., **110**, 1107-1120.

Thomson D.J. (1987). Criteria for the selection of stochastic models of particle trajectories in turbulent flows. *J. Fluid Mech*., **180**, 529-556.

Thomson D.J. (1990). A stochastic model for the motion of particle pairs in isotropic high-Reynolds-number turbulence and its application to the problem of concentration variance. *J. Fluid Mech*., **210**, 113-153.

Thomson, D.J., and Montgomery, M.R., (1994). Reflection boundary conditions for random walk models of dispersion in non-Gaussian turbulence. *Atmospheric Environment*, **28**:1981-1987.

Thomson, D.J., Physick, W.L., and Maryon, R.H., (1997). Treatment of interfaces in random walk dispersion models. *J. Appl. Meteor.*, **36**(9), 1284-1295.

Tinarelli G., Anfossi D., Brusasca G., Ferrero E., Giostra U., Morselli M.G., Moussafir J., Tampieri F. and Trombetti F. (1994). Lagrangian particle simulation of tracer dispersion in the lee of a schematic two-dimensional hill. *J. Appl. Meteor.*, **33**, No. 6, 744-756.

Tinarelli G., Anfossi D., Bider M., Ferrero E. and Trini Castelli S. (2000). A new high performance version of the Lagrangian particle dispersion model SPRAY, some case studies. *Air Pollution Modeling and its Application XIII*, Gryning S.E. and Batchvarova E. Eds.

TRC (1986). Urban Power Plant plume studies. *EPRI Report* EA-5468, EPRI, 3412 Hillview Ave, Palo Alto, Ca 94304

Tremback C.J., Lyons W.A., Thorson W.P. and Walko R.L. (1993). An emergency response and local weather forecasting software system. *Air Pollution and its Application X*, 423-429.

Trini Castelli S. and Anfossi D., (1997). Intercomparison of 3D turbulence parameterisations for dispersion models in complex terrain derived from a circulation model, *Il Nuovo Cimento*, **20 C**, 3, 287-313.

Trini Castelli S. (2000). MIRS: a turbulence parameterisation model interfacing RAMS and SPRAY in a transport and diffusion modelling system. *Int. Rep. ICGF/CNR* No 412/2000.

Uliasz, M. (1994). Lagrangian particle dispersion modelling. In: *Environmental Modeling, Vol II*, Computational Mechanics Publications, Southampton.

van Dop H., Nieuwstadt F.T.M. and Hunt J.C.R. (1985). Random walk models for particle displacements in inhomogeneous unsteady turbulent flows, *Phys. Fluids*, **28**, 1639-1653.

van Dop H. and Nodop K. Guest Eds. (1998). ETEX, a European Tracer Experiment. *Atmospheric Environment*, Vol. 32, no. 24, December 1998, 4089-4378. (S.-E. Gryning and M. M. Millan), Plenum Press, New York, pp.315–323.

van Ulden, A.P. and Holtslag, A. A. M. (1985). Estimation of atmospheric boundary layer parameters for diffusion applications. *J. Clim. And Appl. Meteorol.*, **24**, 1196-1207.

Vinter Falk A.K. (1998). Footprint analysis from random walk models for atmospheric dispersion. Ph.D. Thesis, Technical University of Denmark, Dept of Mathematics, 98 pp.

Wang, L.-P., and D.E. Stock, (1992). Stochastic Trajectory Models for Turbulent Diffusion: Monte-Carlo Process versus Markov Chains. *Atmospheric Environment*, **9**, 1599-1607.

Weil J.C. (1990). A diagnosis of the asymmetry in top-down and bottom-up diffusion using a Lagrangian stochastic model, *J. Atmos. Sci*., **47**, 501-515.

Weil, J. C., (1994). A hybrid Lagrangian dispersion model for elevated sources in the convective boundary layer. *Atmospheric Environment* **28**, 3433–3448.

Willis G.E. and J. Deardorf (1976). A laboratory model of diffusion into the convective planetary boundary layer. *Quart.J.Roy. Meteorol.* Soc., **102**, 427-445.

Willis G.E. and J. Deardorf (1978). A laboratory study of dispersion from an elevated source within a modeled convective planetary boundary layer. *Atmospheric Environment*, **12**, 1305-1311.

Willis G.E. and J. Deardorf (1981). A laboratory study of dispersion from a source in the middle of the convective mixed boundary layer. *Atmospheric Environment*, **15**, 109-117.

Willis G. and J. Deardorff (1983). On plume rise within a convective boundary layer, *Atmospheric Environment*, **17**, 2435-2447.

Willis G. and J. Deardorff (1987). Buoyant plume dispersion and entrapment in and above a laboratory mixed layer, *Atmospheric Environment*, **21**, 1725-1735.

Wilson, K.D. (1997). A three-dimensional correlation/spectral model for turbulent velocities in a convective boundary layer. *Boundary Layer Meteorology,* **85**, 35-52.

Wilson R. B., Start G.E., Dickson C. R. and Ricks N.R. (1976). Diffusion under low wind speed conditions near Oak Ridge, Tennessee. NOAA Technical Memorandum, ERL ARL-61.

Wilson J., G. Thurtell and G. Kidd (1981). Numerical simulation of particle trajectories in inhomogeneous turbulence, II: systems with variable turbulent velocity scale, *Boundary Layer Meteorology,* **21**, 423-441.

Wilson J.D., Legg B.J. and Thomson D.J. (1983). Calculation of particle trajectories in the presence of a gradient in turbulent-velocity variance. *Boundary Layer Meteorology,* **27**, 163-169.

Wilson, J. D. and G.E. Swaters (1991). The source area influencing a measurement in the planetary boundary layer: the "footprint" and the "distribution of contact distance". *Boundary Layer Meteorology,* **55**, 25–46.

Wilson J.D. and Flesch T.K. (1993). Flow boundaries in random-flight dispersion models: enforcing the well-mixed condition. *J. Appl. Meteor.*, **32**, 1695-1707.

Wilson J.D., Thurtell G.W. and Kidd G.E. (1981). Numerical simulation of particle trajectories in inhomogeneous turbulence Part II: Systems with variable turbulence velocity scale. *Boundary Layer Meteorology*, **21**, 423-441.

Wyngaard, J.C., Cote, O.R. and Rao, K.S. (1974). Modelling of the atmospheric boundary layer, Adv. in Geophys., **18A**, Academic Press, 193-212.

Yamada, T. (1985). Numerical simulations of the night 2 data of the 1980 ASCOT experiments in the California Geysers area. *Archiv. for Meteorol., Geophys. and Bioclim.*, **34**, 223-247.

Yamada, T., and S.S. Bunker (1988). Development of a nested grid, second moment turbulence closure model and application to the 1982 ASCOT Brush Creek data simulation. *J. Appl. Meteor*., **27**:562-578.

Yee, E. and Wilson, D. J., (2000). A comparison of the detailed structure in dispersing tracer plumes measured in grid-generated turbulence with a meandering plume model incorporating internal fluctuations. *Boundary Layer Meteorology,* **94**, 253–296.

Zannetti P. (1981). An improved puff algorithm for plume dispersion simulation. *J. Appl. Meteor*.,20, 1023-1211.

Zannetti P. (1984). New Monte Carlo scheme for simulating Lagrangian particle diffusion with wind shear effects. Appl. Math. Modeling, **8**, 188-192.

Zannetti P. (1990). *Air pollution modeling. Theories, Computational Methods and Available Software*. Van Nostrand Reinhold, New York.

Zilitinkevich, S.S. (1972). On the determination of the height of the Ekman boundary layer. *Boundary Layer Meteorology*, **3**, 141-145.